

Novel 5-substituted, 2,4-diaminofuro[2,3-*d*]pyrimidines as multireceptor tyrosine kinase and dihydrofolate reductase inhibitors with antiangiogenic and antitumor activity[☆]

Aleem Gangjee,^{a,*} Yibin Zeng,^{a,†} Michael Ihnat,^b Linda A. Warnke,^b Dixy W. Green,^b Roy L. Kisliuk^c and Fu-Tyan Lin^d

^aDivision of Medicinal Chemistry, Graduate School of Pharmaceutical Sciences, Duquesne University, 600 Forbes Avenue, Pittsburgh, PA 15282, USA

^bDepartment of Cell Biology, The University of Oklahoma Health Science Center, Oklahoma City, OK 73104, USA

^cDepartment of Biochemistry, School of Medicine, Tufts University, Boston, MA 02111, USA

^dDepartment of Chemistry, University of Pittsburgh, Pittsburgh, PA 15213, USA

Received 7 June 2004; accepted 25 April 2005

Available online 21 July 2005

Abstract—Recent evidence suggests that combination therapy of cancer with receptor tyrosine kinase (RTK) inhibitors, which are usually cytostatic, with conventional chemotherapeutic agents, which are usually cytotoxic, provide an improved treatment option. We have designed, synthesized, and evaluated a series of novel 2,4-diamino-5-substituted furo[2,3-*d*]pyrimidines with RTK and dihydrofolate reductase (DHFR) inhibitory activity in single molecules, as potential cytostatic and cytotoxic agents with antitumor activity. These compounds were synthesized from 2,4-diamino-5-chloromethyl furo[2,3-*d*]pyrimidine and aryl methyl ketones using the Wittig reaction to afford the C-8–C-9 unsaturated analogs followed by catalytic reduction to the corresponding saturated compounds. The saturated and unsaturated C-8–C-9 bridged compounds were evaluated as inhibitors of vascular endothelial growth factor receptor (VEGFR-2, Flk, KDR), epidermal growth factor receptor, and platelet-derived growth factor receptor- β (PDGFR- β). Selected analogs were also evaluated as antiangiogenic agents in the chicken embryo chorioallantoic membrane (CAM) assay. The compounds were also evaluated as inhibitors of human (h) DHFR and *Toxoplasma gondii* (tg) DHFR. In each evaluation, a known standard compound was used as a comparison. Of the compounds evaluated, compound **32** was as potent as the standard compounds against VEGFR-2 and PDGFR- β , showing dual inhibitory activity against RTK. This analog was also highly effective in the CAM assay. A second analog **18** also demonstrated dual VEGFR-2 and PDGFR- β inhibitory activity as well as potent antiangiogenic activity in the CAM assay. Four additional analogs were also effective against PDGFR- β and in the CAM assay. An unsaturated C-8–C-9 moiety was necessary for RTK inhibitory activity. Compound **32** also showed inhibitory activity against hDHFR and tgDHFR, illustrating the multitarget inhibitory potential of these analogs. The biological activity of these analogs also suggests the necessity of an unsaturated C-8–C-9 bridge for dual RTK and DHFR inhibitory activity. Compounds **18** and **32** were also evaluated in a B16 melanoma mouse model and were found to be more active as antitumor agents than methotrexate. In addition, both **18** and **32** were also active in decreasing lung metastases in a mouse model of B16 melanomas.

© 2005 Elsevier Ltd. All rights reserved.

1. Introduction

The formation of new blood vessels from existing vasculature is termed angiogenesis.¹ Angiogenesis plays a crucial role in the growth and metastasis of solid tumors.^{2–4} Solid tumors require angiogenesis to grow beyond 1–2 mm in diameter and metastasis requires the presence of blood vessels to allow access to the circulation and to form tumors at distal sites to the primary tumor. Angiogenesis and metastasis contribute to the poor prognosis in patients with angiogenic solid tumors.⁵ Thus, agents that inhibit the angiogenic process have afforded new

[☆] Presented in part at the 218th American Chemical Society National Meeting, New Orleans, LA, August 1999, MEDI 223; and the 94th American Association for Cancer Research National Meeting, Washington, DC, July 2003, Abstract number 101368.

* Corresponding author. Tel.: +1 412 396 6070; fax: +1 412 396 5593; e-mail: gangjee@duq.edu

[†] Present address: Department of Medicinal Chemistry, University of Kansas, Lawrence, KS 66045, USA.

paradigms for the treatment of tumors.^{6,7} Angiogenesis is primarily a receptor-mediated process by growth factors that cause signal transduction, for the most part, via receptor tyrosine kinases (RTK). RTKs consist of families of growth factor receptors such as vascular endothelial growth factor receptor (VEGFR), epidermal growth factor receptor (EGFR), platelet-derived growth factor receptor (PDGFR), and fibroblast growth factor receptor (FGFR) among several others.⁸ Aberrant expression or overexpression of EGFR and PDGFR, both of which are directly or indirectly involved in angiogenesis, have been implicated in the development, progression, and aggressiveness of a variety of solid tumors. These include head and neck cancers,⁹ non-small cell lung cancer,^{10,11} glial tumors,¹² and glioblastomas.^{12–14} VEGF is a known survival factor for endothelial cells of tumor vessels.^{15–23}

RTKs are generally transmembrane receptors consisting of an extracellular growth factor binding domain, a hydrophobic transmembrane domain, and a cytoplasmic domain. The cytoplasmic domain contains regulatory regions and the catalytic tyrosine kinase domain with binding sites for both ATP and substrates allowing for autophosphorylation critical for signal transduction and angiogenesis.^{7,8} Thus, RTKs are attractive targets for cancer chemotherapeutic agents. Since RTKs are present in endothelial cells (VEGFR, PDGFR), tumor cells (FGFR, PDGFR), and pericytes/smooth muscle cells (FGFR, PDGFR), inhibition of more than one RTK could provide synergistic inhibitory effects against solid tumors.^{24–26} Several small molecule RTK inhibitors are currently in clinical use and in clinical trials as antitumor agents (Fig. 1). The majority of these are targeted at the ATP binding sites of tyrosine kinases. The recent approval of Tarceva (OSI774) and Iressa (ZD1839), both of which are EGFR kinase inhibitors, for clinical use against non-small cell lung cancer as well as Gleevec (STI571) against chronic myeloid leukemia and gastrointestinal stromal tumors has established small molecule RTK inhibitors in the clinic as antitumor agents.

There has been considerable discussion in the literature regarding the use of RTK inhibitors as monotherapy for cancer or the combination of multiple RTK inhibitors either as single agents or in combination. In addition, combinations of antiangiogenic agents or RTK inhibitors with conventional cytotoxic cancer chemotherapeutic agents have also been discussed.^{5,22–30} Clinical trials of such combinations are in progress (see website, Cancer Trials at NCI). On the basis of pre-clinical evidence it appears that the primary effect of antiangiogenic agents is cytostatic and that removal of the agent leads to a regrowth of the tumor. In pre-clinical studies, inhibition of multiple RTKs has shown increase in survival in mice.²⁴ There is agreement in the literature that the use of RTK inhibitors (or multiple RTK inhibitors) along with a cytotoxic or conventional cancer chemotherapeutic agents and/or radiation should enhance the efficacy of the overall antitumor therapy and prevent regrowth following cessation of therapy.^{30,31}

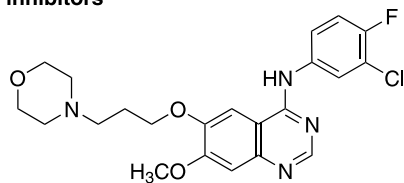
Since RTK inhibitors are generally cytostatic against tumors and the combination of RTK inhibitors with cytotoxic agents, currently in clinical trials, are anticipated to provide better efficacy against tumors, we reasoned that the combination of an RTK inhibitor along with cytotoxic activity in a single molecule could provide single agents with 'combination chemotherapeutic potential' with both cytotoxic and cytostatic activity. Because of our long-standing interest in dihydrofolate reductase (DHFR) inhibitors we elected to use DHFR as the cytotoxic target.

Dihydrofolate reductase (DHFR) carries out the reduction of dihydrofolate to tetrahydrofolate (THF), which is utilized by serinehydroxymethyltransferase to afford 5,10-methylene-tetrahydrofolate (5,10-CH₂THF). The cofactor 5,10-CH₂THF serves as the source of the methyl group in the conversion of deoxyuridine monophosphate (dUMP) to thymidylate (dTMP) catalyzed by thymidylate synthase (TS). DHFR inhibitors are well-established cytotoxic agents used in cancer chemotherapy.^{32,33} Methotrexate (MTX) and trimetrexate (TMQ) (Fig. 1) are examples of such classical and non-classical antifolates, respectively.³⁴

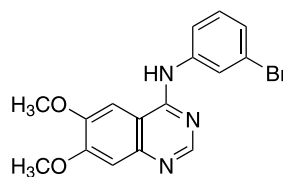
Since inhibition of two or more RTKs have also been proposed to provide synergistic effects when used in combination, it was of interest to structurally engineer single molecules that would possess inhibitory activity against two or more RTKs along with DHFR inhibition. Such analogs were expected to display both cytostatic (RTK inhibition) as well as cytotoxic (DHFR inhibition) activity. Single agents would overcome the pharmacokinetic and pharmacodynamic drawbacks as well as combined toxicities of using two or more separate agents. Recently, VEGFR-2 and PDGFR- β , two RTKs, have been implicated in controlling angiogenesis at two different stages of the angiogenic process, and it has been recently shown that inhibition of VEGFR-2 and PDGFR- β with two separate inhibitors, SU5416 and SU6668, respectively, produces a synergistic effect in early stage as well as late stage pancreatic islet cancer in mouse models by attacking the angiogenic process at two different sites.^{35,36} Thus, we elected to design our multitargeted inhibitor(s) to inhibit DHFR and VEGFR-2 and to evaluate our compounds against PDGFR- β as well.

2,4-Diamino-5-substituted furo[2,3-*d*]pyrimidines **1–16** (Fig. 2), by virtue of their structural analogy to TMQ and molecular modeling, were designed as potential DHFR inhibitors. These analogs have a C–C bridge between the furo[2,3-*d*]pyrimidine and the side chain phenyl ring. The Wittig reaction of 2,4-diamino-5-chloromethyl furo[2,3-*d*]pyrimidine with appropriate aryl methyl ketones was expected to also afford the unsaturated precursors **17–35** (Fig. 2) to the target compounds. Similar unsaturated analogs^{37a,b} have shown DHFR inhibition and would allow the control of side chain conformation in the *E*- and *Z*-isomers for biological activity against the target enzymes. The unsaturated precursors on reduction were to afford the target DHFR inhibitors. Since we desired to combine DHFR and

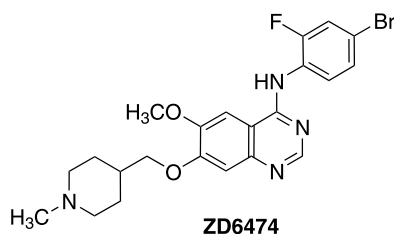
RTK inhibitors



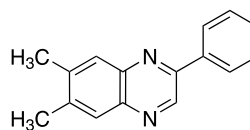
ZD1839 (Iressa)



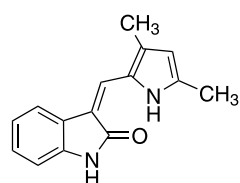
PD153035



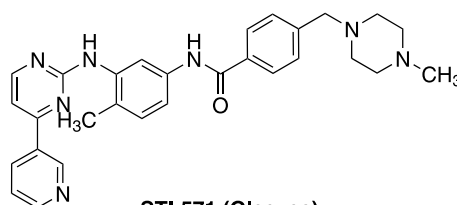
ZD6474



AG1295

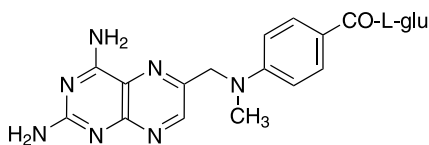


SU5416

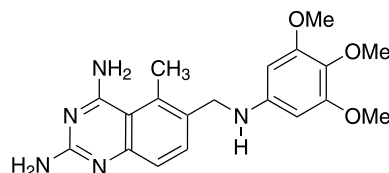


STI-571 (Gleevec)

DHFR inhibitors

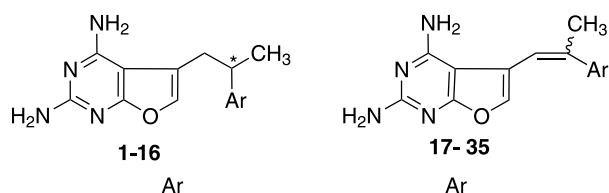


MTX



TMQ

Figure 1. RTK inhibitors and DHFR inhibitors.



1. Phenyl
2. 2-OMe-Phenyl
3. 3-OMe-Phenyl
4. 2-Cl-Phenyl
5. 4-Cl-Phenyl
6. 2,5-diOMe-Phenyl
7. 3,4-diOMe-Phenyl
8. 2,4-diCl-Phenyl
9. 2,5-diCl-Phenyl
10. 3,4-diCl-Phenyl
11. 3,4,5-triOMe-Phenyl
12. 2,3,4-triCl-Phenyl
13. 2-naphthyl
14. 6-OMe-2-naphthyl
15. 4-biphenyl
16. 2-fluorenyl

17. Phenyl
18. 2-OMe-Phenyl
19. 3-OMe-Phenyl
20. 2-Cl-Phenyl
21. 3-Cl-Phenyl
22. 4-Cl-Phenyl
23. 2,4-diOMe-Phenyl
24. 2,5-diOMe-Phenyl
25. 3,4-diOMe-Phenyl
26. 2,4-diCl-Phenyl
27. 2,5-diCl-Phenyl
28. 3,4-diCl-Phenyl
29. 3,4,5-triOMe-Phenyl
30. 2,3,4-triCl-Phenyl
31. 1-naphthyl
32. 2-naphthyl
33. 6-OMe-2-naphthyl
34. 4-biphenyl
35. 2-fluorenyl

Figure 2. Target compounds.

RTK inhibitory activity in single molecules we modeled the potential 2,4-diamino-5-substituted furo[2,3-*d*]pyrimidine DHFR inhibitors into the VEGFR-2 model with ATP (see below). Both the target compounds and the unsaturated precursors were used in the modeling studies.

2. Molecular modeling

The X-ray crystal structure of VEGFR-2 tyrosine kinase has been published.³⁸ Using this crystal structure and sequence homology alignment (SYBYL 6.9)³⁹ with the X-ray crystal structure of insulin receptor kinase (IRK)⁴⁰ containing an ATP bound molecule, it was possible to place the ATP in the VEGFR-2 tyrosine kinase.

Compound **32**, in its energy minimized conformation (SYBYL 6.9) of both the *Z*- and *E*-isomers serves as the prototype and were aligned on the ATP in VEGFR-2 such that the 4-aminopyrimidine moieties of ATP and **32** were superimposed. This allowed a possible binding mode of **32** in VEGFR-2. Figures 3 and 4 indicate that both the *Z*- and *E*-isomers in their energy min-

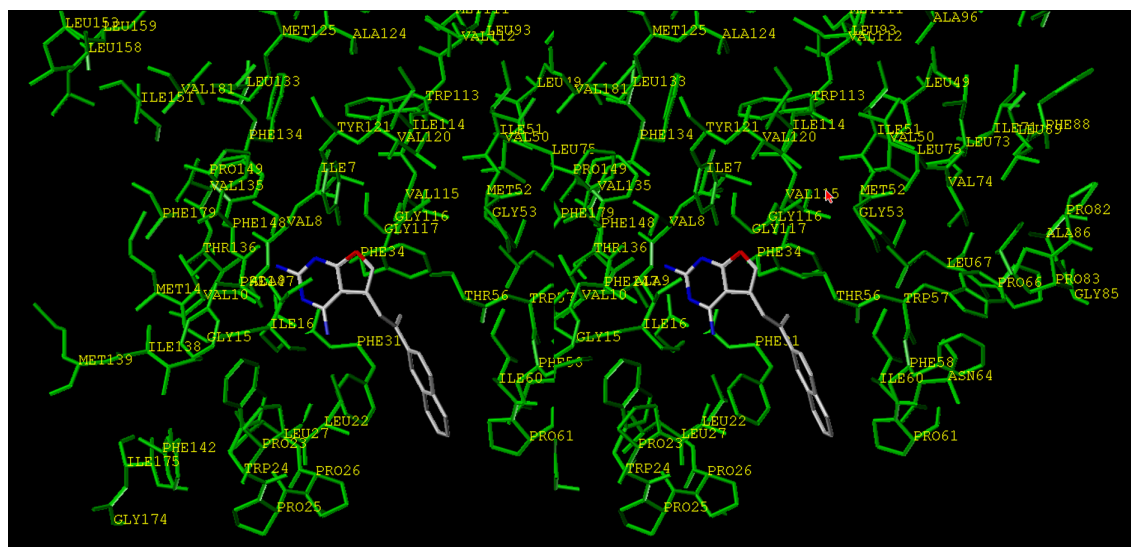
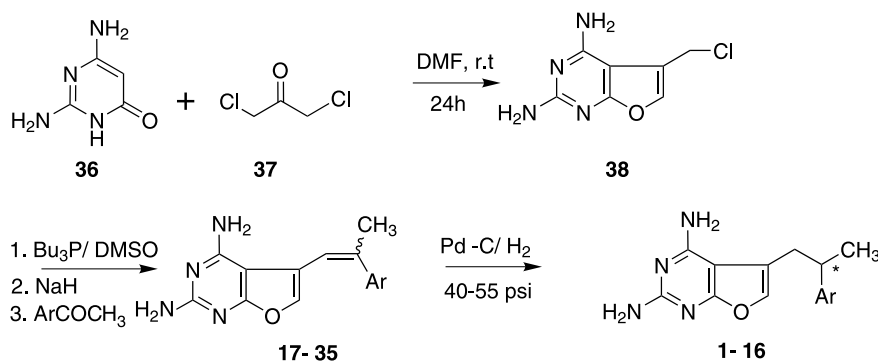


Figure 6. Stereoview of compound *E*-32 modeled in hDHFR in an alternate binding mode to that of *Z*-32.



Scheme 1.

The semistable ylide derived from the 5-chloromethyl furo[2,3-*d*]pyrimidine theoretically ensures a mixture of *E*- and *Z*-isomers for the resulting alkenes,⁴³ thus, it was difficult to synthetically control the *E/Z* ratio. Using lithium free, aprotic, polar DMSO as the solvent at room temperature afforded the *E*-isomer (18–40%) in greater amount than the *Z*-isomer (0–24%).^{44a} In general, attempts to separate the *E/Z* mixtures were extremely tedious. Repeated flash chromatographic separations followed by recrystallization resulted, in some cases, in partial separation of the pure *E*-isomer. The *Z*-isomer either could not be obtained free of *E*-isomer or was obtained in very poor yields (<5%). In one instance for the *E*- and *Z*-2',5'-dichlorophenyl analogs (**27** and **27a**) and in the other instance for the *E*- and *Z*-2,6-dimethoxyphenyl analogs only analytic amounts were obtained.

Hydrogenation of compounds **17–35** in CH₃OH/CHCl₃ afforded the desired target compounds **1–16** as racemic mixtures with yields that varied from 50 to 80%. However, for compounds **21**, **23**, and **31**, due to the formation of the overreduced 5,6-dihydro byproducts, during reduction, they could not be obtained in the pure form without byproduct contamination, even after several rounds of column chromatography. Increased reac-

tion times and/or hydrogen pressures resulted in further reduction of the 5,6-bond of the furan ring.

Compounds **1–35** were evaluated as inhibitors of VEGFR-2 (Flk-1, KDR), EGFR, and PDGFR- β . Selected analogs were also evaluated in the chicken embryo chorioallantoic membrane (CAM) assay for antiangiogenic activity (Table 1). The experimental methods for evaluation were as described by Gangjee et al.⁴¹ Since the IC₅₀ values of the same compound varies under different biological assay conditions,^{44b} we used a standard (control) compound in each of the evaluations to provide a valid comparison with the synthesized analogs. For VEGFR-2, the standard was SU5416, for EGFR the standard was PD153035, and for PDGFR- β the standard was AG1295. SU5416 was also used as the standard for the antiangiogenic activity in the CAM assay.

The saturated compounds **1–16** were inactive in the RTK assays. Interestingly, the corresponding C-8=C-9 conformationally restricted precursor *E*- and *Z*-isomers, analogs **18**, **21**, **30b**, and **32** demonstrated inhibitory activity against VEGFR-2 and **18**, **29**, and **32** were active against PDGFR- β . In addition, these compounds were

Table 1. RTKs inhibitory data and antiangiogenic activity IC₅₀ (μM)⁴¹

Compound	<i>E/Z</i> ratio	EGFR kinase inhibition	VEGFR-2 kinase inhibition	PDGFR-β kinase inhibition	CAM angiogenesis inhibition
18	<i>E</i> -isomer	>50	12.8	10.3	0.08
21	<i>E</i> -isomer	>50	35.8	>50	0.19
22	4:1	>50	>50	>50	
24	<i>E</i> -isomer	>50	>50	>50	
26	<i>E</i> -isomer	>50	>50	>50	
27	<i>E</i> -isomer	>50	>50	>50	
27a	<i>Z</i> -isomer	>50	>50	>50	
28	3:2	>50	>50	>50	
29	2:1	>50	>50	31.8	0.37
30a	<i>E</i> -isomer	>50	>50	>50	
30b	4:1	>50	35.8	>50	0.46
32	2:1	>50	2.8	8.6	0.04
34	2:1	>50	>50	>50	
35	<i>E</i> -isomer	>50	>50	>50	
PD153035		0.2			
SU5416			2.4		0.03
AG1295				6.2	

also active in the CAM assay. Notable among these compounds are the *E*-2-methoxyphenyl analog **18** and the (2:1) *E/Z* mixture, 2-naphthyl analog **32**. Both of these analogs demonstrated potent VEGFR-2 as well as PDGFR-β kinase inhibitory activity with IC₅₀ values comparable to the standards SU5416 and AG1295, respectively. The most potent inhibitors of angiogenesis (in the CAM assay) were the 2:1 *E/Z* mixture **32** and the pure *E*-**18** with IC₅₀ values of 40 and 80 nM, respectively, similar to that of the standard SU5416 (IC₅₀ 30 nM). The difference in potency of **18** and **32** against the RTK (IC₅₀ in μM) and in the CAM assay (IC₅₀

40–80 nM) is identical to that found for the standard SU5416. This underscores the fact that angiogenesis is a multifaceted, multicellular, multikinase, and multiprotein activated process and that perhaps other RTKs involved may also be inhibited, thus providing a synergistic effect on the overall angiogenesis process.

Analogs **1–35** were also evaluated as inhibitors of recombinant human (rh) DHFR and recombinant *Toxoplasma gondii* (tg) DHFR, and the results are reported in Table 2. The methods of evaluation were as previously reported.^{45,46} In general, **1–35** were moderately

Table 2. Inhibitory concentration (IC₅₀ μM) and selectivity ratios against tgDHFR vs hDHFR^a

Compound (CH=C(Me))	<i>E/Z</i> ratio	hDHFR	tgDHFR	h/tg	Compound (CH ₂ CH(Me))	hDHFR	TgDHFR	h/tg
17	2:1	40	30	1.3	1	>37 (35%)	37	ND ^b
18	<i>E</i> -isomer	>34	11	>3	2	>33 (31%)	33	ND ^b
19	2:1	34	10	3.4	3	>34 (22%)	28	ND ^b
20	<i>E</i> -isomer	>33	12	>3	4	31	11	2.8
21	<i>E</i> -isomer	33	1.5	22				
22	4:1	35	11	3.2	5	>33 (26%)	40	ND ^b
23	<i>E</i> -isomer	30	11	2.7				
24	<i>E</i> -isomer	>31	15	>2	6	>30 (38%)	15	ND ^b
25	2:1	20	27	0.74	7	30	10	3
26	<i>E</i> -isomer	35	10	3.5	8	29	2.9	10
27	<i>E</i> -isomer	30	10	3	9	>10 (39%)	15	ND ^b
27a	<i>Z</i> -isomer	25	14	1.8				
28	3:2	20	1.7	11.8	10	30	5	6
29	2:1	28	25	1.1	11	270	27	10
30a	<i>E</i> -isomer	>27	27	ND	12	>10 (37%)	5	ND ^b
30b	4:1	25	1.7	14.7				
31	<i>E</i> -isomer	30	0.3	100				
32	2:1	10	0.3	33	13	16	11	1.5
33	2:1	25	0.3	83	14	>28 (22%)	28	ND ^b
34	2:1	20	0.3	67	15	25	7	3.6
35	<i>E</i> -isomer	ND ^b	ND ^b	ND ^b	16	23	10	2.3
					TMP	>350 (28%)	17	>20
					MTX	0.02	0.02	1

DHFR assay conditions: all enzymes were assayed spectrophotometrically in a solution containing 50 M dihydrofolate, 80 M NADPH, 0.05 M Tris-HCl, 0.001 M 2-mercaptoethanol, and 0.001 M EDTA at pH 7.4 and 30 °C. The reaction was initiated with an amount of enzyme yielding a change in OD at 340 nM of 0.015 min⁻¹.

^a Recombinant hDHFR was provided by Dr. J.H. Freisheim. Recombinant tgDHFR was provided by Dr. D.V. Santi.

^b ND, not determined.

active as inhibitors of rhDHFR and tgDHFR with IC_{50} values in the range 10^{-7} – 10^{-6} M. Interestingly, they inhibited tgDHFR to a greater extent than rhDHFR. Some of the geometrically restricted, bicyclic side chain analogs **31**–**34** showed higher potency and remarkable selectivity ratios (IC_{50} h/tg) of 33–100 against tgDHFR. The most potent rhDHFR inhibitor was analog **32** with an IC_{50} of 10 μ M. There was no major difference in the *E*- and *Z*-isomers in DHFR inhibitory potency where the *E*- and *Z*-isomers were separated (compound **27**). The results suggest that, for 2,4-diamino-5-substituted-furo[2,3-*d*]pyrimidines, the side chain substitution pattern may be more important than the geometric orientation for DHFR inhibition.

To examine whether compounds **18** and **32** were effective in vivo in reducing tumor volume and metastasis, a syngeneic mouse tumor model was used. This model is a widely accepted model for testing tumor growth and metastases.⁴⁷ The B16 model of tumor growth produces almost quantitative (100%) tumor take in a very short time after administration,^{48,49} so animals are not wasted. The B16 tumor cells are skin-derived, so subcutaneous implantation is adequate and resulting tumors are superficial and easily measured, and the B16-F10 variant used in these studies is highly metastatic and most if not all metastases go to the lung, making metastasis evaluation very facile.^{48–51} Unlike most human tumor xenograft models, the B16 model produces highly vascularized tumors so that the effect of tumor-mediated angiogenesis can be evaluated.^{48–51} For these studies, animals were implanted with green fluorescent protein (GFP) tagged B16-F10 cells.⁴⁷ One week after implantation, animals were treated biweekly with 25 mg/kg methotrexate or 25 mg/kg compounds **18** or **32** intraperitoneally. Primary tumor volume was measured and the tumor rates were calculated as in the Section 5. The results of the compounds on primary tumor growth rates are shown in Figure 7. Methotrexate, compound **18**, and compound **32** all resulted in a significant ($P < 0.005$) decrease in primary tumor growth rate as compared to untreated animals. In addition, compounds **18** and **32** resulted in a significant ($P < 0.05$) reduction in growth rate as compared to methotrexate treatment. Lung metastases was measured by staining for GFP, an exogenous protein, and the results are shown in Figure 8. All three drugs (methotrexate, **18**, and **32**) resulted in a significant ($P < 0.05$) decrease in the number of lung metastases per lobe. In this case, however, there was no significant decrease in lung metastases with **18** or **32** as compared with methotrexate, although a trend toward significance was present. The increased activity of **18** and **32** in the in vivo antitumor evaluation, compared to methotrexate could be the result of a synergistic effect of RTK inhibition along with DHFR inhibitory activity. For a synergistic effect the individual drugs need not be highly potent. Thus, even the low hDHFR inhibitory activity of both **18** and **32** perhaps act in concert with the RTK inhibitory activity to provide a viable antitumor effect in vivo against B16 melanoma.

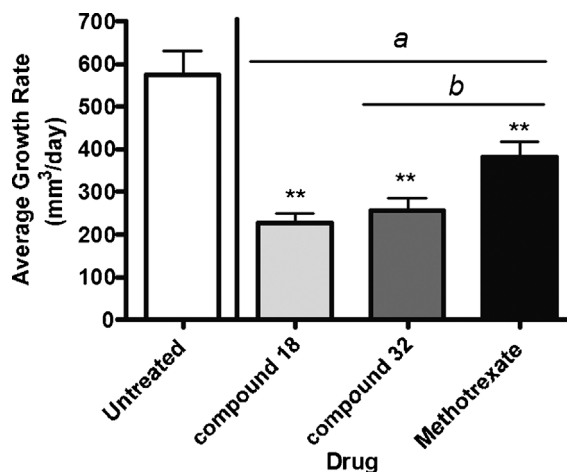


Figure 7. Effect of methotrexate, compound **18**, and compound **32** on growth of B16-10 primary tumors. Mice bearing B16-F10 GFP-tagged tumors were treated biweekly with 25 mg/kg drug and tumors measured biweekly as in Section 5. Tumor growth rates were calculated using linear regression analysis in Prism 4.0 software. Data represent means \pm SEM from 5 to 9 animals. * $P < 0.05$, ** $P < 0.005$ as compared to untreated animals; a = $P < 0.005$, b = $P < 0.05$ as compared with methotrexate-treated animals using two-way ANOVA with Dunnett's post-test.

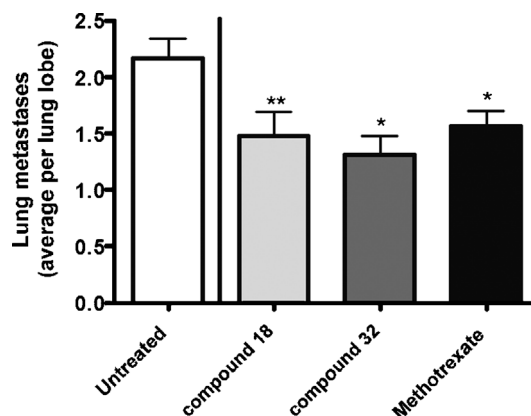


Figure 8. Effect of methotrexate, compound **18**, and compound **32** on growth of B16-10 lung metastases. Mice bearing B16-F10 GFP-tagged tumors were treated biweekly with 25 mg/kg drug and tumors measured biweekly as in Section 5. Tumor growth rates were calculated using linear regression analysis in Prism 4.0 software. Data represent means \pm SEM from 5 to 9 animals. * $P < 0.05$, ** $P < 0.005$ as compared to untreated animals using one-way ANOVA with Bonferroni's multiple comparison post-test.

4. Conclusion

In summary, a series of 5-substituted, 2,4-diamino-furo[2,3-*d*]pyrimidines were designed and synthesized as a novel class of multitarget inhibitors of RTKs, which also exhibit DHFR inhibitory activity. These analogs were designed with the potential to possess both cytostatic activity (RTK inhibition) and cytotoxic activity (DHFR inhibition) in a single molecule. Several of the unsaturated bridge analogs synthesized not only possess good inhibitory activity against VEGFR-2 and PDGFR- β that were similar to that of the standard

compounds SU5416 and AG1295, respectively, but also maintain moderate DHFR inhibitory activity. Several of these compounds also showed potent antiangiogenic activity in the CAM assay similar to the standard SU5416. The results suggest that the nature of the side chain aromatic substituent plays an important role in the inhibitory activity against RTKs and DHFR. Compound **32** serves as a lead analog for rationally designed RTK inhibitory activity combined with DHFR inhibitory activity in a single molecule. Efforts are currently underway to improve the DHFR inhibitory activity using **32** as the lead analog. The *in vivo* antitumor evaluation of **18** and **32** suggest that both compounds **18** and **32** are active as antitumor agents *in vivo*, both against primary tumors and metastases, and are both at least as active against B16 melanomas as the standard drug, methotrexate.

5. Experimental

All evaporations were carried out *in vacuo* with a rotary evaporator. Analytical samples were dried *in vacuo* (0.2 mm Hg) in a CHEM-DRY drying apparatus over P₂O₅ at 80 °C. Melting points were determined on a MEL-TEMP II melting point apparatus with FLUKE 51 K/J electronic thermometer and are uncorrected. Nuclear magnetic resonance spectra for proton (¹H NMR) were recorded on a Bruker WH-300 (300 MHz) spectrometer. The chemical shift values are expressed in ppm (parts per million) relative to tetramethylsilane as an internal standard: s, singlet; d, doublet; t, triplet; q, quartet; m, multiplet; br, broad singlet. The relative integrals of peak areas agreed with those expected for the assigned structures. NOESY, COSY experiments were performed on a Bruker DRX500 (500 MHz) spectrometer. Thin-layer chromatography (TLC) was performed on POLYGRAM Sil G/UV254 silica gel plates with a fluorescent indicator, and the spots were visualized under 254 and 366 nm illumination. Proportions of solvents used for TLC are by volume. Column chromatography was performed on a 230–400 mesh silica gel purchased from Aldrich, Milwaukee, WI. Elemental analyses were performed by Atlantic Microlab, Inc., Norcross, GA. Element compositions are within 0.4% of the calculated values. Fractional moles of water or organic solvents frequently found in some analytical samples of antifolates could not be prevented in spite of 24–48 h of drying *in vacuo* and were confirmed where possible by their presence in the ¹H NMR spectra. All solvents and chemicals were purchased from Aldrich Chemical Co. or Fisher Scientific and were used as received.

5.1. General procedure for the synthesis of 17–35

To a solution of 2,4-diamino-5-(chloromethyl)furo[2,3-*d*]pyrimidine, **38**, (1.0 g, 5 mmol) in anhydrous DMSO (15 mL) was added tributylphosphine (92%, 1.7 g 7.5 mmol), and the resulting mixture was stirred at 60 °C in an oil bath for 3 h under N₂ to form the phosphonium salt. The deep orange solution was then cooled to room temperature. To this solution was added

sodium hydride (90% dispersion in mineral oil, 0.2 g, 6 mmol), followed by the desired commercially available aryl methyl ketone (5.5 mmol). The reaction mixture was stirred at room temperature for 24–32 h. TLC showed the disappearance of the starting 2,4-diamino-5-(chloromethyl)-furo[2,3-*d*]pyrimidine and the formation of two (olefinic) spots. The reaction was quenched with 20 mL methanol, washed with two portions of 50 mL methanol, and the resulting solution was evaporated under reduced pressure to dryness. To the residue was added 6 g of silica gel and CHCl₃ (25 mL) and the slurry was loaded onto a 4 × 20 cm dry silica gel column and flash chromatographed initially with CHCl₃ (300 mL), then sequentially with 2% MeOH in CHCl₃ (250 mL), 5% CH₃OH in CHCl₃ (300 mL), and 10% CH₃OH in CHCl₃ (250 mL). Fractions which showed the desired spot on TLC were pooled and evaporated to dryness and the residue was recrystallized from ethylacetate to afford the desired olefinic targets **17–35**.

5.1.1. *E/Z*-2,4-Diamino-5-[2-(phenyl)propenyl]furo[2,3-*d*]pyrimidine (17). Compound **38** (1.0 g, 5 mmol) and acetophenone (660 mg, 5.5 mmol) for 24 h afforded **17** (400 mg, 30%) as yellow crystals: mp 230.8–233.8 °C; *R_f* = 0.59 and 0.54 (CHCl₃/CH₃OH 5:1); ¹H NMR (DMSO-*d*₆) (*E/Z* = 2:1) *E*-isomer δ 2.22 (s, 3H, 9-CH₃), 6.07 (s, 2H, 4-NH₂), 6.45 (s, 2H, 2-NH₂), 6.88 (s, 1H, 8-CH), 7.29–7.40 (m, 3H, C₆H₅), 7.46 (s, 1H, 6-CH), 7.62–7.65 (d, 2H, C₆H₅); *Z*-isomer δ 2.10 (s, 3H, 9-CH₃), 5.99 (s, 2H, 4-NH₂), 6.23 (s, 1H, C-8-CH), 6.49 (s, 2H, 2-NH₂), 6.59 (s, 1H, 6-CH), 7.18–7.40 (m, 5H, C₆H₅). Anal. (C₁₅H₁₄N₄O) C, H, N.

5.1.2. *E*-2,4-Diamino-5-[2-(2'-methoxyphenyl)propenyl]furo[2,3-*d*]pyrimidine (18). Compound **38** (1.0 g, 5 mmol) and 2'-methoxyacetophenone (830 mg, 5.5 mmol) for 32 h afforded **18** (350 mg, 25%) as orange crystals: mp 191.3–193.3 °C; *R_f* = 0.54 (CHCl₃/CH₃OH 5:1); ¹H NMR (DMSO-*d*₆): δ 2.07 (s, 3H, 9-CH₃), 3.80 (s, 3H, OMe), 6.08 (s, 2H, 4-NH₂), 6.42 (s, 2H, 2-NH₂), 6.48 (s, 1H, 8-CH), 6.93–7.11 (m, 2H, C₆H₄), 7.26–7.42 (d, 2H, C₆H₄), 7.47 (s, 1H, 6-CH). Anal. (C₁₆H₁₆N₄O₂) C, H, N.

5.1.3. *E/Z*-2,4-Diamino-5-[2-(3'-methoxyphenyl)propenyl]furo[2,3-*d*]pyrimidine (19). Compound **38** (1.0 g, 5 mmol) and 3'-methoxyacetophenone (830 mg, 5.5 mmol) for 30 h afforded **19** (400 mg, 27%) as yellow needles: mp 193.2–197.8 °C; *R_f* = 0.55 and 0.50 (CHCl₃/CH₃OH 5:1); ¹H NMR (DMSO-*d*₆) (*E/Z* = 2:1) *E*-isomer δ 2.20 (s, 3H, 9-CH₃), 3.80 (s, 3H, OMe), 6.07 (s, 2H, 4-NH₂), 6.45 (s, 2H, 2-NH₂), 6.88–6.89 (t, 2H, C-8-CH and C₆H₄), 7.18–7.32 (d, 3H, C₆H₄), 7.45 (s, 1H, 6-CH); *Z*-isomer δ 2.17 (s, 3H, 9-CH₃), 3.75 (s, 3H, OMe), 6.00 (s, 2H, 4-NH₂), 6.36 (s, 1H, C-8-CH), 6.52 (s, 1H, 6-CH), 6.57 (s, 2H, 2-NH₂), 6.73–6.89 (m, 3H, C₆H₄), 7.14–7.18 (m, 1H, C₆H₄). Anal. (C₁₆H₁₆N₄O₂·0.25H₂O) C, H, N.

5.1.4. *E*-2,4-Diamino-5-[2-(2'-chlorophenyl)propenyl]furo[2,3-*d*]pyrimidine (20). Compound **38** (1.0 g, 5 mmol) and 2'-chloroacetophenone (850 mg, 5.5 mmol) for 24 h afforded **20** (500 mg, 33%) as yellow crystals: mp

234.5–236.4 °C (dec); $R_f = 0.58$ (CHCl₃/CH₃OH 5:1); ¹H NMR (DMSO-*d*₆) *E*-isomer δ 2.20 (s, 3H, 9-CH₃), 6.15 (s, 2H, 4-NH₂), 6.50 (s, 2H, 2-NH₂), 6.66 (s, 1H, 8-CH), 7.39–7.54 (m, 4H, C₆H₄), 7.58 (s, 1H, 6-CH). Anal. (C₁₅H₁₃N₄OCl) C, H, N, Cl.

5.1.5. *E*-2,4-Diamino-5-[2-(3'-chlorophenyl)propenyl]furo[2,3-*d*]pyrimidine (21). Compound **38** (1.0 g, 5 mmol) and 3'-chloroacetophenone (850 mg, 5.5 mmol) for 24 h afforded **21** along with its *Z*-isomer (550 mg, 37%) as yellow needles: mp 210.6–215.7 °C (dec); $R_f = 0.58$ and 0.54 (CHCl₃/CH₃OH 5:1); ¹H NMR (DMSO-*d*₆) (*E/Z* = 2:1); *E*-isomer δ 2.21 (s, 3H, 9-CH₃), 6.08 (s, 2H, 4-NH₂), 6.54 (s, 2H, 2-NH₂), 6.92 (s, 1H, 8-CH), 7.35–7.43 (m, 2H, C₆H₄), 7.48 (s, 1H, 6-CH), 7.57–7.60 (d, 1H, C₆H₄), 7.73 (s, 1H, C₆H₄); *Z*-isomer δ 2.17 (s, 3H, 9-CH₃), 6.02 (s, 2H, 4-NH₂), 6.36 (s, 2H, 2-NH₂), 6.54 (s, 1H, 8-CH), 6.62 (s, 1H, 6-CH), 7.43–7.13 (m, 4H, C₆H₄). Anal. (C₁₅H₁₃N₄OCl) C, H, N, Cl.

The above mixture was reloaded for another round of flash column chromatography and afforded the pure *E*-isomer **21** (150 mg, 11%) as light yellow needles: mp 215.6–218.7 °C; $R_f = 0.58$ (CHCl₃/CH₃OH 5:1); ¹H NMR (DMSO-*d*₆): δ 2.21 (s, 3H, 9-CH₃), 6.08 (s, 2H, 4-NH₂), 6.54 (s, 2H, 2-NH₂), 6.92 (s, 1H, 8-CH), 7.35–7.43 (m, 2H, C₆H₄), 7.48 (s, 1H, 6-CH), 7.57–7.60 (d, 1H, C₆H₄), 7.73 (s, 1H, C₆H₄). Anal. (C₁₅H₁₃N₄OCl) C, H, N, Cl.

5.1.6. *E/Z*-2,4-Diamino-5-[2-(4'-chlorophenyl)propenyl]furo[2,3-*d*]pyrimidine (22). Compound **38** (1.0 g, 5 mmol) and 4'-chloroacetophenone (850 mg, 5.5 mmol) for 24 h afforded **22** (600 mg, 40%) as yellow needles: mp 247.5–252.5 °C; $R_f = 0.61$ and 0.58 (CHCl₃/CH₃OH 5:1); ¹H NMR (DMSO-*d*₆) (*E/Z* = 4:1) *E*-isomer δ 2.20 (s, 3H, 9-CH₃), 6.09 (s, 2H, 4-NH₂), 6.52 (s, 2H, 2-NH₂), 6.88 (s, 1H, 8-CH), 7.44–7.39 (d, 2H, C₆H₄), 7.47 (s, 1H, 6-CH), 7.66–7.69 (d, 2H, C₆H₄); *Z*-isomer δ 2.17 (s, 3H, 9-CH₃), 6.02 (s, 2H, 4-NH₂), 6.38 (s, 1H, 8-CH) 6.44 (s, 2H, 2-NH₂), 6.61 (s, 1H, 6-CH), 7.20–7.23 (d, 2H, C₆H₄), 7.35–7.38 (d, 2H, C₆H₄). Anal. (C₁₅H₁₃N₄OCl) C, H, N, Cl.

5.1.7. *E*-2,4-Diamino-5-[2-(2',4'-dimethoxyphenyl)propenyl]furo[2,3-*d*]pyrimidine (23). Compound **38** (1.0 g, 5 mmol) and 2',4'-dimethoxyacetophenone (1.0 g, 5.5 mmol) for 32 h afforded **23** (300 mg, 18%) as yellow needles: mp 210.3–211.6 °C; $R_f = 5.7$ (EtOH/EtOAc 1:2); ¹H NMR (DMSO-*d*₆): δ 2.04 (s, 3H, 9-CH₃), 3.77 (s, 3H, 4'-OCH₃), 3.79 (s, 3H, 2'-OCH₃), 6.08 (s, 2H, 4-NH₂), 6.39 (s, 2H, 2-NH₂), 6.44 (s, 1H, C₆H₃), 6.58 (s, 1H, C₆H₃), 6.59 (s, 1H, 8-CH), 7.19 (s, 1H, C₆H₃), 7.45 (s, 1H, 6-CH). Anal. (C₁₇H₁₈N₄O₃) C, H, N.

5.1.8. *E*-2,4-Diamino-5-[2-(2',5'-dimethoxyphenyl)propenyl]furo[2,3-*d*]pyrimidine (24). Compound **38** (1.0 g, 5 mmol) and 2',5'-dimethoxyacetophenone (1.0 g, 5.5 mmol) for 32 h afforded **24** (250 mg, 15%) as yellow needles: mp 178.5–179.9 °C; $R_f = 0.68$ (CHCl₃/CH₃OH 5:1); ¹H NMR (DMSO-*d*₆): δ 2.06 (s, 3H, 9-CH₃), 3.72 (s, 3H, OMe), 3.74 (s, 3H, OMe), 6.08 (s, 2H, 4-NH₂), 6.44 (s, 2H, 2-NH₂), 6.51 (s, 1H, 8-CH), 6.82–6.85

(m, 2H, C₆H₃), 6.95–6.97 (d, 1H, C₆H₃), 7.41 (s, 1H, 6-CH); Anal. (C₁₇H₁₈N₄O₃) C, H, N.

A (5:2) *E/Z* mixture (200 mg) was also obtained: mp 170.9–179.9 °C; $R_f = 0.68$ and 0.65 (CHCl₃/CH₃OH 5:1); total yield 28%. ¹H NMR (DMSO-*d*₆) *E*-isomer δ 2.06 (s, 3H, 9-CH₃), 3.72 (s, 3H, OMe), 3.74 (s, 3H, OMe), 6.08 (s, 2H, 4-NH₂), 6.44 (s, 2H, 2-NH₂), 6.51 (s, 1H, 8-CH), 6.82–6.85 (m, 2H, C₆H₃), 6.95–6.97 (d, 1H, C₆H₃), 7.41 (s, 1H, 6-CH); *Z*-isomer δ 2.10 (s, 3H, 9-CH₃), 3.65 (s, 6H, OMe), 5.98 (s, 2H, 4-NH₂), 6.17 (s, 1H, 8-CH), 6.44 (s, 2H, 2-NH₂), 6.55–6.56 (d, 1H, C₆H₃), 6.60 (s, 1H, 6-CH), 6.82–6.86 (dd, 2H, C₆H₃). Anal. (C₁₇H₁₈N₄O₃) C, H, N.

5.1.9. *E/Z*-2,4-Diamino-5-[2-(3',4'-dimethoxyphenyl)propenyl]furo[2,3-*d*]pyrimidine (25). Compound **38** (1.0 g, 5 mmol) and 3',4'-dimethoxyacetophenone (1.0 g, 5.5 mmol) for 32 h afforded **25** (480 mg, 29%) as a white powder: mp 232–251 °C (dec); $R_f = 0.52$ and 0.49 (CHCl₃/CH₃OH 5:1); ¹H NMR (DMSO-*d*₆) (*E/Z* = 2:1) *E*-isomer δ 2.18 (s, 3H, 9-CH₃), 3.77 (s, 3H, OMe), 3.82 (s, 3H, OMe), 6.06 (s, 2H, 4-NH₂), 6.47 (s, 2H, 2-NH₂), 6.79 (s, 1H, 8-CH), 7.13–7.16 (d, 2H, C₆H₃), 7.20 (s, 1H, C₆H₃), 7.41 (s, 1H, 6-CH); *Z*-isomer δ 2.16 (s, 3H, 9-CH₃), 3.59 (s, 3H, OMe), 3.72 (s, 3H, OMe), 5.98 (s, 2H, 4-NH₂), 6.42 (s, 2H, 2-NH₂), 6.50 (s, 1H, 8-CH), 6.76 (s, 1H, 6-CH), 6.86–6.95 (m, 3H, C₆H₃). Anal. (C₁₇H₁₈N₄O₃) C, H, N.

5.1.10. *E*-2,4-Diamino-5-[2-(2',4'-dichlorophenyl)propenyl]furo[2,3-*d*]pyrimidine (26). Compound **38** (1.0 g, 5 mmol) and 2',4'-dichloroacetophenone (1.05 g, 5.5 mmol) for 24 h afforded **26** (850 mg, 50%) as yellow needles: mp 220.8–223.2 °C; $R_f = 0.63$ (CH₂Cl/CH₃OH 5:1); ¹H NMR (DMSO-*d*₆): δ 2.12 (s, 3H, 9-CH₃), 6.09 (s, 2H, 4-NH₂), 6.49 (s, 2H, 2-NH₂), 6.61 (s, 1H, 8-CH), 7.69–7.43 (m, 4H, C₆H₃ and C6-CH). Anal. (C₁₅H₁₂N₄OCl₂) C, H, N, Cl.

5.1.11. *E*-2,4-Diamino-5-[2-(2',5'-dichlorophenyl)propenyl]furo[2,3-*d*]pyrimidine (27). Compound **38** (1.0 g, 5 mmol) and 2',5'-dichloroacetophenone (1.05 g, 5.5 mmol) for 24 h afforded **27** (410 mg, 24%) as yellow needles: mp 229.5–231.5 °C; $R_f = 0.69$ (CHCl₃/CH₃OH 5:1); ¹H NMR (DMSO-*d*₆): δ 2.13 (s, 3H, 9-CH₃), 6.09 (s, 2H, 4-NH₂), 6.51 (s, 2H, 2-NH₂), 6.64 (s, 1H, 8-CH), 7.39–7.42 (dd, 1H, C₆H₃), 7.50–7.54 (m, 3H, 6-CH and C₆H₃). Anal. (C₁₅H₁₂N₄OCl₂) C, H, N, Cl.

A mixture of **27** and its *Z*-isomer **27a** (270 mg, total) was also obtained as yellow crystals: mp 225–232.8 °C; $R_f = 0.69$ and 0.62 (CHCl₃/CH₃OH 5:1); ¹H NMR (DMSO-*d*₆) *E*-isomer δ 2.13 (s, 3H, 9-CH₃), 6.09 (s, 2H, 4-NH₂), 6.51 (s, 2H, 2-NH₂), 6.64 (s, 1H, 8-CH), 7.39–7.42 (dd, 1H, C₆H₃), 7.50–7.54 (m, 3H, 6-CH and C₆H₃); *Z*-isomer δ 2.13 (s, 3H, 9-CH₃), 6.03 (s, 2H, 4-NH₂), 6.10 (s, 1H, 8-CH), 6.63 (s, 2H, 2-NH₂), 6.80 (s, 1H, 6-CH), 7.33–7.53 (m, 3H, C₆H₃); total yield 41%.

5.1.12. *Z*-2,4-Diamino-5-[2-(2',5'-dichlorophenyl)propenyl]furo[2,3-*d*]pyrimidine (27a). The above mixture was reloaded for additional two rounds of flash column

chromatography and afforded the pure **Z-27a** (70 mg, 4%) as yellow crystals: mp: 253.6–255.8 °C; $R_f = 0.60$ (CHCl₃/CH₃OH 5:1); ¹H NMR (DMSO-*d*₆): δ 2.13 (s, 3H, 9-CH₃), 6.03 (s, 2H, 4-NH₂), 6.10 (s, 1H, 8-CH), 6.63 (s, 2H, 2-NH₂), 6.80 (s, 1H, 6-CH), 7.33–7.53 (m, 3H, C₆H₃). Anal. (C₁₅H₁₂N₄OCl₂) C, H, N, Cl.

5.1.13. *E/Z*-2,4-Diamino-5-[2-(3',4'-dichlorophenyl)propenyl]furo[2,3-*d*]pyrimidine (28). Compound **38** (1.0 g, 5 mmol) and 3',4'-dichloroacetophenone (1.05 g, 5.5 mmol) for 24 h afforded **28** (1.12 g, 63%) as a white powder: mp 232.6–236.6 °C; $R_f = 0.57$ and 0.55 (CHCl₃/CH₃OH 5:1); ¹H NMR (DMSO-*d*₆) (*E/Z* = 3:2) *E*-isomer δ 2.20 (s, 3H, 9-CH₃), 6.08 (s, 2H, 4-NH₂), 6.57 (s, 2H, 2-NH₂), 6.94 (s, 1H, 8-CH), 7.49 (s, 1H, 6-CH), 7.62 (s, 2H, C₆H₃), 7.93 (s, 1H, C₆H₃); *Z*-isomer δ 2.17 (s, 3H, 9-CH₃), 6.03 (s, 2H, 4-NH₂), 6.51 (s, 2H, 2-NH₂), 6.57 (s, 1H, 8-CH), 6.63 (s, 1H, 6-CH), 7.16–7.15 (d, 1H, C₆H₃), 7.47 (s, 1H, C₆H₃), 7.56–7.53 (d, 1H, C₆H₃). Anal. (C₁₅H₁₂N₄OCl₂) C, H, N, Cl.

5.1.14. *E/Z*-2,4-Diamino-5-[2-(3',4',5'-trimethoxyphenyl)propenyl]furo[2,3-*d*]pyrimidine (29). Compound **38** (1.0 g, 5 mmol) and 3',4',5'-trimethoxyacetophenone (1.16 g, 5.5 mmol) for 28 h afforded **29** (1.0 g, 42%) as yellow needles: mp 198–207 °C; $R_f = 0.48$ and 0.43 (CHCl₃/CH₃OH 7:1); ¹H NMR (DMSO-*d*₆) (*E/Z* = 2:1) *E*-isomer δ 2.20 (s, 3H, 9-CH₃), 3.67 (s, 3H, 4'-OCH₃), 3.83 (s, 6H, 3',5'-OCH₃), 6.07 (s, 2H, 4-NH₂), 6.43 (s, 2H, 2-NH₂), 6.81 (s, 1H, 8-CH), 6.85 (s, 2H, C₆H₂), 7.44 (s, 1H, 6-CH); *Z*-isomer δ 2.18 (s, 3H, 9-CH₃), 3.57 (s, 9H, OCH₃), 5.99 (s, 2H, 4-NH₂), 6.45 (s, 2H, 2-NH₂), 6.50 (s, 3H, 8-CH and C₆H₂), 6.55 (s, 1H, 6-CH). Anal. (C₁₈H₂₀N₄O₄) C, H, N.

5.1.15. *E*-2,4-Diamino-5-[2-(2',3',4'-trichlorophenyl)propenyl]furo[2,3-*d*]pyrimidine (30a). Compound **38** (1.0 g, 5 mmol) and 2',3',4'-chloroacetophenone (1.25 g, 5.5 mmol) for 28 h and after two rounds of flash column chromatography afforded **30a** (130 mg, 8%) as a white powder: mp 265.2–266.5 °C, $R_f = 0.57$ (CHCl₃/CH₃OH 5:1); ¹H NMR (DMSO-*d*₆) *E*-isomer δ 2.13 (s, 3H, 9-CH₃), 6.07 (s, 2H, 4-NH₂), 6.49 (s, 2H, 2-NH₂), 6.64 (s, 1H, 8-CH), 7.39–7.42 (d, 1H, C₆H₂), 7.56 (s, 1H, 6-CH), 7.65–7.68 (d, 1H, C₆H₂); Anal. (C₁₅H₁₁N₄OCl₃) C, H, N, Cl.

5.1.16. *E/Z*-2,4-Diamino-5-[2-(2',3',4'-trichlorophenyl)propenyl]furo[2,3-*d*]pyrimidine (30b). The above procedure also afforded **30b** (800 mg, 42%) as a light yellow powder: mp 260.6–265.6 °C; $R_f = 0.55$ and 0.57 (CHCl₃/CH₃OH 5:1) (*E/Z* 4:1) ¹H NMR (DMSO-*d*₆) *E*-isomer δ 2.13 (s, 3H, 9-CH₃), 6.07 (s, 2H, 4-NH₂), 6.49 (s, 2H, 2-NH₂), 6.64 (s, 1H, 8-CH), 7.39–7.42 (d, 1H, C₆H₂), 7.56 (s, 1H, 6-CH), 7.65–7.68 (d, 1H, C₆H₂); *Z*-isomer δ 2.54 (s, 3H, 9-CH₃), 6.03 (s, 2H, 4-NH₂), 6.51 (s, 2H, 2-NH₂), 6.57 (s, 1H, 8-CH), 6.63 (s, 1H, 6-CH), 7.15–7.16 (d, 1H, C₆H₂), 7.53–7.56 (d, 1H, C₆H₂). Anal. (C₁₅H₁₁N₄OCl₃) C, H, N, Cl.

5.1.17. *E*-2,4-Diamino-5-[2-(1'-naphthyl)propenyl]furo[2,3-*d*]pyrimidine (31). Compound **38** (1.0 g, 5 mmol) and 1'-acetonaphthone (940 mg, 5.5 mmol) for 28 h

afforded **31** (320 mg, 22%) as yellow needles: mp 232.8–235 °C (dec); $R_f = 0.41$ (CHCl₃/CH₃OH 8:1); ¹H NMR (DMSO-*d*₆) δ 2.28 (s, 3H, 9-CH₃), 6.08 (s, 2H, 4-NH₂), 6.40 (s, 2H, 2-NH₂), 6.70 (s, 1H, 8-CH), 7.44–7.54 (m, 3H, C₁₀H₇), 7.64 (s, 1H, 6-CH), 7.86–7.95 (m, 4H, C₁₀H₇). Anal. (C₁₉H₁₆N₄O·0.25H₂O) C, H, N.

5.1.18. *E/Z*-2,4-Diamino-5-[2-(2'-naphthyl)propenyl]furo[2,3-*d*]pyrimidine (32). Compound **38** (1.0 g, 5 mmol) and 2'-acetonaphthone (940 mg, 5.5 mmol) for 28 h afforded **32** (480 mg, 30%) as yellow needles: mp 238.2–247.5 °C; $R_f = 0.55$ and 0.52 (CHCl₃/CH₃OH 5:1); ¹H NMR (DMSO-*d*₆) (*E/Z* = 2:1) *E*-isomer δ 2.34 (s, 3H, 9-CH₃), 6.09 (s, 2H, 4-NH₂), 6.52 (s, 2H, 2-NH₂), 7.05 (s, 1H, 8-CH), 7.51–7.49 (m, 3H, 6-CH and C₁₀H₇), 7.96–7.89 (m, 4H, C₁₀H₇), 8.09 (s, 1H, C₁₀H₇); *Z*-isomer δ 2.26 (s, 3H, 9-CH₃), 5.99 (s, 2H, 4-NH₂), 6.29 (s, 1H, 8-CH), 6.54 (s, 2H, 2-NH₂), 6.67 (s, 1H, 6-CH), 7.13–7.17 (m, 3H, C₁₀H₇), 7.70–7.89 (m, 4H, C₁₀H₇). Anal. (C₁₉H₁₆N₄O) C, H, N.

5.1.19. *E/Z*-2,4-Diamino-5-[2-(6'-methoxy-2'-naphthyl)propenyl]furo[2,3-*d*]pyrimidine (33). Compound **38** (1.0 g, 5 mmol) and 2-acetyl-6-methoxynaphthalene (1.05 g, 5.5 mmol) for 28 h afforded **33** (540 mg, 31%) as a white powder: mp 254.4–257.8 °C (dec); $R_f = 0.7$ and 0.67 (CHCl₃/CH₃OH 5:1); ¹H NMR (DMSO-*d*₆) (*E/Z* = 2:1) *E*-isomer δ 2.31 (s, 3H, 9-CH₃), 3.88 (s, 3H, OMe), 6.07 (s, 2H, 4-NH₂), 6.49 (s, 2H, 2-NH₂), 7.00 (s, 1H, 8-CH), 7.24–7.32 (m, 2H, C₁₀H₆), 7.48 (s, 2H, 6-CH), 7.81–7.95 (m, 3H, C₁₀H₆), 8.09 (s, 1H, C₁₀H₆); *Z*-isomer δ 2.26 (s, 3H, 9-CH₃), 3.93 (s, 3H, OMe), 5.98 (s, 2H, 4-NH₂), 6.29 (s, 1H, 8-CH), 6.49 (s, 2H, 2-NH₂), 6.64 (s, 1H, 6-CH), 7.13–7.17 (m, 2H, C₁₀H₆), 7.71–7.84 (m, 4H, C₁₀H₆). Anal. (C₂₀H₁₈N₄O₂) C, H, N.

5.1.20. *E/Z*-2,4-Diamino-5-[2-(4'-biphenyl)propenyl]furo[2,3-*d*]pyrimidine (34). Compound **38** (1.0 g, 5 mmol) and 4-phenylacetophenone (1.08 g, 5.5 mmol) for 32 h afforded **34** (550 mg, 30%) as yellow needles: mp 239.8–245.8 °C; $R_f = 0.58$ and 0.53 (CHCl₃/CH₃OH 5:1); ¹H NMR (DMSO-*d*₆) (*E/Z* = 2:1) *E*-isomer δ 2.25 (s, 3H, 9-CH₃), 6.08 (s, 2H, 4-NH₂), 6.50 (s, 2H, 2-NH₂), 6.94 (s, 1H, 8-CH), 7.30–7.47 (m, 4H, C₆H₄), 7.48 (s, 1H, 6-CH), 7.65–7.73 (m, 5H, C₆H₅); *Z*-isomer δ 2.21 (s, 3H, 9-CH₃), 6.01 (s, 2H, 4-NH₂), 6.41 (s, 1H, 8-CH), 6.52 (s, 2H, 2-NH₂), 6.62 (s, 1H, 6-CH), 7.30–7.73 (m, 9H, C₁₂H₉). Anal. (C₂₁H₁₈N₄O) C, H, N.

5.1.21. *E*-2,4-Diamino-5-[2-(2'-fluorenyl)propenyl]furo[2,3-*d*]pyrimidine (35). Compound **38** (1.0 g, 5 mmol) and 2-acetylfluorene (1.15 g, 5.5 mmol) for 32 h afforded **35** (350 mg, 23%) as a yellow powder: mp 279.8–282.2 °C (dec); $R_f = 0.56$ (CHCl₃/CH₃OH 5:1); ¹H NMR (DMSO-*d*₆) δ 2.08 (s, 3H, 9-CH₃), 2.24 (s, 2H, C₁₃H₉), 6.08 (s, 2H, 4-NH₂), 6.59 (s, 2H, 2-NH₂), 7.01 (s, 1H, 8-CH), 7.40–7.35 (m, 1H, C₁₃H₉), 7.49 (s, 1H, 6-CH), 7.64–7.60 (m, 2H, C₁₃H₉), 7.90–7.78 (m, 4H, C₁₃H₉). Anal. (C₂₂H₁₈N₄O) C, H, N.

5.2. General procedure for the synthesis of 1–16

To a solution of the olefinic intermediate (0.3–0.7 mmol) in a mixture of CHCl_3 (50 mL) and CH_3OH (15 mL) was added 5% palladium on activated carbon (0.20 g), and the suspension was hydrogenated in a Parr apparatus at room temperature at 40–55 psi for 3–24 h, TLC indicated the disappearance of the starting material and the formation of one major spot. The reaction mixture was filtered through Celite, washed with 30% CH_3OH in CHCl_3 (3×20 mL). After evaporation of the solvent, CH_3OH (50 mL) was added to afford a solution. To this solution was added 5 g silica gel and the mixture was evaporated under reduced pressure to dryness. The silica gel plug was loaded on a dry silica gel column (2×16 cm) and flash chromatographed initially with CHCl_3 (150 mL), then sequentially with 1% CH_3OH in CHCl_3 (150 mL), 2% CH_3OH in CHCl_3 (150 mL), and 5% CH_3OH in CHCl_3 (150 mL). Fractions which showed the major spot on TLC were pooled and evaporated to dryness. The residue was recrystallized from CH_3OH or other solvent combinations as indicated to afford the desired target compounds 1–16. The yields varied from 50 to 80%.

5.2.1. (R,S)-2,4-Diamino-5-[2-(phenyl)propyl]furo[2,3-*d*]pyrimidine (1). Compound 17 (180 mg, 0.7 mmol) hydrogenated at 40 psi for 3 h afforded 1 (120 mg, 66%) as white needles: mp 257.6–259.6 °C; $R_f = 0.54$ ($\text{CHCl}_3/\text{CH}_3\text{OH}$ 5:1); $^1\text{H NMR}$ ($\text{DMSO-}d_6$): δ 1.22–1.24 (d, 3H, 9- CH_3), 2.90–2.92 (d, 2H, 8- CH_2), 2.93–3.01 (m, 1H, 9-CH), 5.95 (s, 2H, 4- NH_2), 6.39 (s, 2H, 2- NH_2), 6.88 (s, 1H, 6-CH), 7.13–7.30 (m, 5H, C_6H_5). Anal. ($\text{C}_{15}\text{H}_{16}\text{N}_4\text{O}$) C, H, N.

5.2.2. (R,S)-2,4-Diamino-5-[2-(2'-methoxyphenyl)propyl]furo[2,3-*d*]pyrimidine (2). Compound 18 (100 mg, 0.3 mmol) hydrogenated at 45 psi for 3 h afforded 2 (70 mg, 70%) as white needles: mp 182.5–185.1 °C; $R_f = 0.53$ ($\text{CHCl}_3/\text{CH}_3\text{OH}$ 5:1); $^1\text{H NMR}$ ($\text{DMSO-}d_6$): δ 1.13–1.15 (d, 3H, 9- CH_3), 2.46–2.54 (d, 2H, 8- CH_2), 2.88 (m, 1H, 9-CH), 3.80 (s, 3H, OMe), 6.04 (s, 2H, 4- NH_2), 6.57 (s, 2H, 2- NH_2), 6.90–6.99 (m, 2H, C_6H_4), 7.02 (s, 1H, 6-CH), 7.16–7.27 (m, 2H, C_6H_4). Anal. ($\text{C}_{16}\text{H}_{18}\text{N}_4\text{O}_2 \cdot 0.25 \text{H}_2\text{O}$) C, H, N.

5.2.3. (R,S)-2,4-Diamino-5-[2-(3'-methoxyphenyl)propyl]furo[2,3-*d*]pyrimidine (3). Compound 19 (120 mg, 0.4 mmol) hydrogenated at 45 psi for 6 h afforded 3 (75 mg, 62%) as white crystals: mp 186.7–188.5 °C; $R_f = 0.52$ ($\text{CHCl}_3/\text{CH}_3\text{OH}$ 5:1); $^1\text{H NMR}$ ($\text{DMSO-}d_6$): δ 1.21–1.23 (d, 3H, 9- CH_3), 2.90–2.99 (m, 3H, 8- CH_2 and 9-CH), 3.71 (s, 3H, OMe), 5.97 (s, 2H, 4- NH_2), 6.41 (s, 2H, 2- NH_2), 6.71–6.81 (m, 3H, C_6H_4), 6.92 (s, 1H, 6-CH), 7.14–7.19 (t, 1H, C_6H_4). Anal. ($\text{C}_{16}\text{H}_{18}\text{N}_4\text{O}_2$) C, H, N.

5.2.4. (R,S)-2,4-Diamino-5-[2-(2'-chlorophenyl)propyl]furo[2,3-*d*]pyrimidine (4). Compound 20 (150 mg, 0.4 mmol) hydrogenated at 55 psi for 24 h afforded 4 (80 mg, 52%) as white needles: mp 232.2–233.9 °C; $R_f = 0.53$ ($\text{CHCl}_3/\text{CH}_3\text{OH}$ 5:1); $^1\text{H NMR}$ ($\text{DMSO-}d_6$): δ 1.20–1.22 (d, 3H, 9- CH_3), 2.96–2.98 (d, 2H, 8- CH_2),

3.48–3.55 (m, 1H, 9-CH), 5.97 (s, 2H, 4- NH_2), 6.45 (s, 2H, 2- NH_2), 6.94 (s, 1H, 6-CH), 7.16–7.51 (m, 4H, C_6H_4). Anal. ($\text{C}_{15}\text{H}_{15}\text{N}_4\text{OCl} \cdot 0.5 \text{CH}_3\text{OH}$) C, H, N, Cl.

5.2.5. (R,S)-2,4-Diamino-5-[2-(4'-chlorophenyl)propyl]furo[2,3-*d*]pyrimidine (5). Compound 22 (100 mg, 0.3 mmol) hydrogenated at 50 psi for 5 h afforded 5 (60 mg, 60%) as white crystals: mp 249.7–252.5 °C. $R_f = 0.57$ ($\text{CHCl}_3/\text{CH}_3\text{OH}$ 5:1); $^1\text{H NMR}$ ($\text{DMSO-}d_6$): δ 1.21–1.23 (d, 3H, 9- CH_3), 2.90–2.92 (d, 2H, 8- CH_2), 2.96–3.02 (m, 1H, 9-CH), 5.96 (s, 2H, 4- NH_2), 6.41 (s, 2H, 2- NH_2), 6.88 (s, 1H, 6-CH), 7.23–7.32 (dd, 4H, C_6H_4). Anal. ($\text{C}_{15}\text{H}_{15}\text{N}_4\text{OCl}$) C, H, N, Cl.

5.2.6. (R,S)-2,4-Diamino-5-[2-(2',5'-dimethoxyphenyl)propyl]furo[2,3-*d*]pyrimidine (6). Compound 24 (100 mg, 0.3 mmol) hydrogenated at 45 psi for 6 h afforded 6 (50 mg, 50%) as yellow crystals: mp 171.6–173.6 °C. $R_f = 0.56$ ($\text{CHCl}_3/\text{CH}_3\text{OH}$ 5:1); $^1\text{H NMR}$ ($\text{DMSO-}d_6$): δ 1.29–1.31 (d, 3H, 9- CH_3), 2.98–3.00 (d, 2H, 8- CH_2), 3.09–3.17 (m, 1H, 9-CH), 3.65 (s, 6H, OMe), 6.02 (s, 2H, 4- NH_2), 6.44 (s, 2H, 2- NH_2), 6.55–6.56 (d, 1H, C_6H_3), 6.82–6.90 (m, 2H, C_6H_3), 6.92 (s, 1H, C-6-CH). Anal. ($\text{C}_{17}\text{H}_{20}\text{N}_4\text{O}_3 \cdot 0.2\text{H}_2\text{O}$) C, H, N.

5.2.7. (R,S)-2,4-Diamino-5-[2-(3',4'-dimethoxyphenyl)propyl]furo[2,3-*d*]pyrimidine (7). Compound 25 (100 mg, 0.3 mmol) hydrogenated at 45 psi for 3 h afforded 7 (50 mg, 50%) as white crystals: mp 198.7–201.2 °C; $R_f = 0.52$ ($\text{CHCl}_3/\text{CH}_3\text{OH}$ 5:1); $^1\text{H NMR}$ ($\text{DMSO-}d_6$): δ 1.20–1.22 (d, 3H, 9- CH_3), 2.83–2.97 (m, 3H, 8- CH_2 , 9-CH), 3.68 (s, 3H, 4'-O CH_3), 3.70 (s, 3H, 3'-O CH_3), 5.97 (s, 2H, 4- NH_2), 6.40 (s, 2H, 2- NH_2), 6.69–6.72 (d, 1H, C_6H_3), 6.79–6.81 (t, 2H, C_6H_3), 6.91 (s, 1H, 6-CH). Anal. ($\text{C}_{17}\text{H}_{20}\text{N}_4\text{O}_3 \cdot 0.5 \text{H}_2\text{O}$) C, H, N.

5.2.8. (R,S)-2,4-Diamino-5-[2-(2',4'-dichlorophenyl)propyl]furo[2,3-*d*]pyrimidine (8). Compound 26 (100 mg, 0.3 mmol) hydrogenated at 50 psi for 16 h afforded 8 (65 mg, 65%) as white needles (recrystallized from $\text{Et}_2\text{O}/\text{CH}_3\text{OH}$): mp 220.5–223.1 °C; $R_f = 0.58$ ($\text{CHCl}_3/\text{CH}_3\text{OH}$ 5:1). $^1\text{H NMR}$ ($\text{DMSO-}d_6$): δ 1.20–1.22 (d, 3H, 9- CH_3), 2.90–3.05 (d, 2H, 8- CH_2), 3.30–3.35 (m, 1H, 9-CH), 5.96 (s, 2H, 4- NH_2), 6.45 (s, 2H, 2- NH_2), 6.86 (s, 1H, 6-CH), 7.40–7.52 (m, 3H, C_6H_3). Anal. ($\text{C}_{15}\text{H}_{14}\text{N}_4\text{OCl}_2 \cdot 0.075\text{Et}_2\text{O}$) C, H, N, Cl.

5.2.9. (R,S)-2,4-Diamino-5-[2-(2',5'-dichlorophenyl)propyl]furo[2,3-*d*]pyrimidine (9). Compound 27 (120 mg, 0.28 mmol) hydrogenated at 50 psi for 20 h afforded 9 (60 mg, 50%) as white needles (recrystallized from cyclohexane/ CH_3OH): mp 246.7–248.6 °C; $R_f = 0.57$ ($\text{CHCl}_3/\text{CH}_3\text{OH}$ 5:1); $^1\text{H NMR}$ ($\text{DMSO-}d_6$): δ 1.20–1.22 (d, 3H, 9- CH_3), 2.96–3.04 (br, 2H, 8- CH_2), 3.17–3.19 (br, 1H, 9-CH), 5.96 (s, 2H, 4- NH_2), 6.47 (s, 2H, 2- NH_2), 6.92 (s, 1H, 6-CH), 7.27–7.28 (m, 1H, C_6H_3), 7.38 (s, 1H, C_6H_3), 7.58–7.57 (d, 1H, C_6H_3). Anal. ($\text{C}_{15}\text{H}_{14}\text{N}_4\text{OCl}_2 \cdot 0.05\text{C}_6\text{H}_{12}$) C, H, N, Cl.

5.2.10. (R,S)-2,4-Diamino-5-[2-(3',4'-dichlorophenyl)propyl]furo[2,3-*d*]pyrimidine (10). Compound 28 (150 mg, 0.4 mmol) hydrogenated at 50 psi for 14 h afforded 10 (80 mg, 52%) as white needles: mp 187.2–189.2 °C;

$R_f = 0.55$ (CHCl₃/CH₃OH 5:1); ¹H NMR (DMSO-*d*₆): δ 1.21–1.23 (d, 3H, 9-CH₃), 2.89–2.91 (br, 2H, 8-CH₂), 2.96–3.03 (br, 1H, 9-CH), 5.96 (s, 2H, 4-NH₂), 6.45 (s, 2H, 2-NH₂), 6.95 (s, 1H, 6-CH), 7.20–7.23 (m, 1H, C₆H₃), 7.48–7.57 (m, 2H, C₆H₃). Anal. (C₁₅H₁₄N₄O-Cl₂·0.05H₂O) C, H, N, Cl.

5.2.11. (R,S)-2,4-Diamino-5-[2-(3',4',5'-trimethoxyphenyl)propyl]furo[2,3-*d*]pyrimidine (11). Compound **29** (120 mg, 0.4 mmol) hydrogenated at 40 psi for 5 h afforded **11** (60 mg, 50%) as white needles: mp 201–203 °C; $R_f = 0.62$ (CHCl₃/CH₃OH 5:1); ¹H NMR (DMSO-*d*₆): δ 1.21 (d, 3H, 9-CH₃), 2.90 (d, 2H, 8-CH₂), 3.16 (m, 1H, 9-CH), 3.64 (s, 3H, 4'-OCH₃), 3.73 (s, 6H, 3', 5'-OCH₃), 5.95 (s, 2H, 4-NH₂), 6.39 (s, 2H, 2-NH₂), 6.52 (s, 2H, C₆H₂), 6.99 (s, 1H, 6-CH). Anal. (C₁₈H₂₂N₄O₄·0.5 H₂O).

5.2.12. (R,S)-2,4-Diamino-5-[2-(2',3',4'-dichlorophenyl)propyl]furo[2,3-*d*]pyrimidine (12). Compound **30** (180 mg, 0.4 mmol) hydrogenated at 55 psi for 22 h afforded **12** (120 mg, 66%) as white crystals (recrystallized from EtOAc): mp 257.6–259.6 °C; $R_f = 0.54$ (CHCl₃/CH₃OH 5:1); ¹H NMR (DMSO-*d*₆): δ 1.27–1.29 (d, 3H, 9-CH₃), 3.04–3.06 (d, 2H, 8-CH₂), 3.22–3.25 (m, 1H, 9-CH), 6.03 (s, 2H, 4-NH₂), 6.54 (s, 2H, 2-NH₂), 6.97 (s, 1H, 6-CH), 7.59–7.56 (d, 1H, C₆H₂), 7.70–7.67 (d, 1H, C₆H₂). Anal. (C₁₅H₁₃N₄OCl₃) C, H, N, Cl.

5.2.13. (R,S)-2,4-Diamino-5-[2-(2'-naphthyl)propyl]furo[2,3-*d*]pyrimidine (13). Compound **32** (100 mg, 0.3 mmol) hydrogenated at 50 psi for 5 h afforded **13** (50 mg, 50%) as white crystals: mp 230.2–232 °C; $R_f = 0.57$ (EtOH/EtOAc/hexane 1:2:1); ¹H NMR (DMSO-*d*₆): δ 1.29–1.31 (d, 3H, 9-CH₃), 2.92–3.10 (m, 3H, 8-CH₂ and 9-CH), 5.95 (s, 2H, 4-NH₂), 6.43 (s, 2H, 2-NH₂), 6.85 (s, 1H, 6-CH), 7.40–7.48 (m, 3H, C₁₀H₇), 7.65 (s, 1H, C₁₀H₇), 7.80–7.85 (m, 3H, C₁₀H₇). Anal. (C₁₉H₁₈N₄O·0.1H₂O) C, H, N.

5.2.14. (R,S)-2,4-Diamino-5-[2-(6'-methoxy-2'-naphthyl)propyl]furo[2,3-*d*]pyrimidine (14). Compound **33** (100 mg, 0.4 mmol) hydrogenated at 50 psi for 22 h afforded **14** (80 mg, 80%) as white crystals (recrystallized from CH₃OH/EtOAc): mp 244–245.9 °C; $R_f = 0.58$ (EtOH/EtOAc/hexane 1:2:1); ¹H NMR (DMSO-*d*₆): δ 1.29–1.31 (d, 3H, 9-CH₃), 2.98–3.02 (d, 2H, 8-CH₂), 3.09–3.17 (m, 1H, 9-CH), 3.83 (s, 3H, OMe), 5.99 (s, 2H, 4-NH₂), 6.39 (s, 2H, 2-NH₂), 6.88 (s, 1H, 6-CH), 7.11–7.08 (t, 1H, C₁₀H₆), 7.24 (d, 1H, C₁₀H₆), 7.37–7.40 (d, 1H, C₁₀H₆), 7.61 (s, 1H, C₁₀H₆), 7.69–7.75 (dd, 2H, C₁₀H₆). Anal. (C₂₀H₂₀N₄O₂·0.25 H₂O) C, H, N.

5.2.15. (R,S)-2,4-Diamino-5-[2-(4'-biphenyl)propyl]furo[2,3-*d*]pyrimidine (15). Compound **34** (120 mg, 0.4 mmol) hydrogenated at 45 psi for 16 h afforded **15** (60 mg, 50%) as white crystals: mp 243.1–245.1 °C; $R_f = 0.52$ (CHCl₃/CH₃OH 5:1); ¹H NMR (DMSO-*d*₆): δ 1.27–1.25 (d, 3H, 9-CH₃), 2.95 (d, 2H, 8-CH₂), 3.18–3.08 (m, 1H, 9-CH), 5.96 (s, 2H, 4-NH₂), 6.42 (s, 2H, 2-NH₂), 6.94 (s, 1H, 6-CH), 7.64–7.32 (m, 9H, C₁₂H₉). Anal. (C₂₁H₂₀N₄O·0.4H₂O) C, H, N.

5.2.16. (R,S)-2,4-diamino-5-[2-(2'-fluorenyl)propyl]furo[2,3-*d*]pyrimidine (16). Compound **35** (100 mg, 0.3 mmol) hydrogenated at 50 psi for 22 h afforded **16** (50 mg, 50%) as yellow crystals (recrystallized from CH₃OH/cyclohexane): mp 250.3–252.2 °C; $R_f = 0.59$ (CHCl₃/CH₃OH 5:1); ¹H NMR (DMSO-*d*₆): δ 1.27–1.29 (d, 3H, 9-CH₃), 2.95–2.97 (d, 2H, 8-CH₂), 3.02–3.17 (m, 1H, 9-CH), 3.86 (s, 2H, C₁₃H₉), 5.95 (s, 2H, 4-NH₂), 6.42 (s, 2H, 2-NH₂), 6.92 (s, 1H, 6-CH), 7.22–7.83 (m, 7H, C₁₃H₉). Anal. (C₂₂H₂₀N₄O·0.15C₆H₁₂) C, H, N.

5.3. Mouse tumor studies

All animal studies were conducted in accordance with AALAC approved guidelines using a protocol approved by the IACUC at the University of Oklahoma. Six-week-old male NCr nu/nu mice (NCI APA breeding stock, Frederick, MD) were housed in ventilated cages with autoclaved chow, water, and bedding. Following one week of acclimation, 5×10^5 B16-F10 (GFP) cells⁴⁷ in 100 μ l PBS/1 μ M EDTA were injected subcutaneously into the external surface at the base of the right ear (where the B16 tumor originally derived; ATCC web site <http://www.atcc.org/>). On days 7, 11, 14, 18, 21, and 25, post-implantation animals received injections of 25 mg/kg methotrexate (Sigma Chemical) or of compounds **18** or **32** intraperitoneally in 100 μ l sterile water/1% DMSO. Animals were assessed for the presence of tumors every other day and tumor measurement began 7 days after implantation and continued biweekly until tumors reached approximately 8–10% of animal body weight (day 28 post-implantation). The length (*L*) and width (*W*) of tumors were measured using Vernier calipers (Mitutoyo, Kawasaki Kanagawa, Japan) and tumor volume calculated using the formula $L \times W^2$.

After killing mice (28 days post-implantation), the tumor and lungs were excised, fixed for 8 h in neutral buffered formalin, embedded in paraffin, sectioned, and stained by either H&E or standard immunohistochemical methods as previously described.⁴⁷ Sections were deparaffinized, incubated in 6% peroxide for 20 min, incubated in 0.1 M sodium citrate until boiling, and then for 10 additional minutes on 30% peroxide using a 700 W microwave oven. Sections were then blocked using Vectastain kits (Vector Laboratories, Burlingame, CA) and then exposed to an antibody against GFP (Clontech) to examine micrometastases. Secondary antibody and ABC reagent were then added and the sections were stained with VIP peroxidase substrate (Vector Laboratories) and counterstained with Gomori trichrome (J.T. Baker Company).⁴⁷

5.3.1. Cells. All cells were maintained at 37 °C in a humidified environment containing 5% CO₂ using media from Mediatech (Hemden, NJ). A-431 cells were from the American Type Tissue Collection (Manassas, VA).

5.3.2. Chemicals. All growth factors (bFGF, VEGF, EGF, and PDGF-BB) were purchased from Peprotech (Rocky Hill, NJ). PD153035, SU5416, AG1295, and

VEGF kinase inhibitor (4-[(4'-chloro-2'-fluoro)phenylamino]-6,7-dimethoxyquinazoline) were purchased from Calbiochem (San Diego, CA). The CYQUANT cells proliferation assay was from Molecular Probes (Eugene, OR). All other chemicals were from Sigma Chemical unless otherwise noted.

5.3.3. Antibodies. The PY-HRP antibody was from BD Transduction Laboratories (Franklin Lakes, NJ). Antibodies against EGFR, PDGFR- β , FGFR-1, Flk-1, and Flt-1 were purchased from Upstate Biotech (Framingham, MA).

5.3.4. Phosphotyrosine ELISA. Cells used were tumor cell lines naturally expressing high levels of EGFR (A431), Flk-1 (U251), Flt-1 (A498), and PDGFR- β (SF-539), and FGFR-1 (NIH OVCAR-8). Expression levels at the RNA level were derived from the NCI Developmental Therapeutics Program (NCI-DTP) web site public molecular target information (http://www.dtp.nci.nih.gov/mtargets/mt_index.html). Briefly, cells at 60–75% confluence are placed in serum-free medium for 18 h to reduce the background of phosphorylation. Cells were always >98% viable by Trypan blue exclusion. Cells are then pretreated for 60 min with 10, 3.33, 1.11, 0.37, and 0.12 μ M compound followed by 100 ng/ml EGF, VEGF, PDGF-BB, or bFGF for 10 min. The reaction is stopped and cells permeabilized by quickly removing the media from the cells and adding ice-cold Tris-buffered saline (TBS) containing 0.05% Triton X-100, protease inhibitor cocktail and tyrosine phosphatase inhibitor cocktail. The TBS solution is then removed and cells fixed to the plate for 30 min at 60 °C and further incubation in 70% ethanol for an additional 30 min. Cells are further exposed to block (TBS with 1% BSA) for 1 h, washed, and then a horseradish peroxidase (HRP)-conjugated phosphotyrosine (PY) antibody added overnight. The antibody is removed, cells are washed again in TBS, exposed to an enhanced luminol ELISA substrate (Pierce Chemical, Rockford, IL) and light emission measured using a UV products (Upland, CA) BioChemi digital darkroom. The known RTK-specific kinase inhibitor PD153035 was used as a positive control compound for EGFR kinase inhibition; SU5416 for Flk1 kinase inhibition; AG1295 for PDGFR- β kinase inhibition; and VEGF kinase inhibitor (4-[(4'-chloro-2'-fluoro)phenylamino]-6,7-dimethoxyquinazoline) was used as a positive control for both Flt1 and Flk1 kinase inhibition. Data were graphed as a percent of cells receiving growth factor alone and IC_{50} values were estimated from two to three separate experiments ($n = 8$ –24) using hand-drawn probit plots. In each case, the activity of a positive control inhibitor did not deviate more than 10% from the IC_{50} values listed in the text.

5.3.5. CYQUANT cell proliferation assay. As a measure of cell proliferation, the CYQUANT cell counting/proliferation assay was used as previously described.⁵² Briefly, cells are first treated with compounds for 12 h and then allowed to grow for an additional 36 h. The cells are then lysed and the CYQUANT dye, which

intercalates into the DNA of cells, is added and after 5 min the fluorescence of each well measured using an UV products BioChemi digital darkroom. A positive control used for cytotoxicity in each experiment was cisplatin, with an apparent average IC_{50} value of $8.2 \pm 0.65 \mu$ M. Data are graphed as a percent of cells receiving growth factor alone and IC_{50} values estimated from two to three separate experiments ($n = 6$ –15) using probit plots.

5.3.6. Chorioallantoic membrane assay of angiogenesis. The chorioallantoic membrane (CAM) assay is a standard assay for testing antiangiogenic agents.⁵³ The CAM assay used in these studies was modified from a procedure by Sheu⁵⁴ and Brooks⁵⁵ and as published previously.⁵⁶ Briefly, fertile leghorn chicken eggs (CBT Farms, Chestertown, MD) are allowed to grow until 10 days of incubation. The proangiogenic factors, human VEGF-165 and bFGF (100 ng each) are then added saturation to a 6 mm microbial testing disk (BBL, Cockeysville, MD) and placed onto the CAM by breaking a small hole in the superior surface of the egg. Antiangiogenic compounds are added 8 h after the VEGF/bFGF at saturation to the same microbial testing disk and embryos allowed to incubate for an additional 40 h. After 48 h, the CAMs are perfused with 2% paraformaldehyde/3% glutaraldehyde containing 0.025% Triton X-100 for 20 s, excised around the area of treatment, fixed again in 2% paraformaldehyde/3% glutaraldehyde for 30 min, placed on petri dishes, and a digitized image taken using a dissecting microscope (Wild M400; Bannockburn, IL) at 7.5X and SPOT enhanced digital imaging system (Diagnostic Instruments, Sterling Heights, MI). A grid is then added to the digital CAM images and the average number of vessels within 5–7 grids counted as a measure of vascularity. AGM-1470 (a kind gift of the NIH Developmental Therapeutics Program) and SU5416 are used as a positive control for antiangiogenic activity. Data are graphed as a percent of CAMs receiving bFGF/VEGF and IC_{50} values estimated from two to three separate experiments ($n = 5$ –11) using probit plots.

5.3.7. Statistics. All analysis was done using Prism 4.0. (GraphPad Software, San Diego, CA). Tumor growth rates were assessed during the linear growth period and statistical significance of tumor growth between groups was calculated using two-way repeated measures ANOVA with treatments and days after implantation as independent variables with Dunnett's post-test with the null hypothesis rejected when $P < 0.05$. Tumor metastases were compared using one-way ANOVA with Bonferonni's multiple comparison post-test with the null hypothesis rejected when $P < 0.05$.

Acknowledgment

This work was supported, in part, by the National Institutes of Health, National Cancer Institute Grants CA09885 (A.G.) and CA10914 (R.L.K.).

Appendix A. Elemental analyses

Compound	Formula	Calcd (%)				Found (%)			
		C	H	N	Cl	C	H	N	Cl
1	C ₁₅ H ₁₆ N ₄ O	67.15	6.01	20.88		67.28	5.97	20.92	
2	C ₁₆ H ₁₈ N ₄ O ₂ ·0.25H ₂ O	64.14	6.08	18.78		63.74	6.04	18.44	
3	C ₁₆ H ₁₈ N ₄ O ₂	64.41	6.08	18.78		64.39	5.99	18.88	
4	C ₁₅ H ₁₅ N ₄ OCl ₂ ·0.5CH ₃ OH	58.40	5.33	17.57	11.12	58.49	5.41	17.53	11.29
5	C ₁₅ H ₁₅ N ₄ OCl	59.51	4.99	18.51	11.71	59.36	5.02	18.32	11.91
6	C ₁₇ H ₂₀ N ₄ O ₃ ·0.2H ₂ O	61.50	6.19	16.87		61.59	6.11	16.80	
7	C ₁₇ H ₂₀ N ₄ O ₃ ·0.5H ₂ O	60.46	6.22	16.60		60.81	6.22	16.67	
8	C ₁₅ H ₁₄ N ₄ OCl ₂ ·0.075Et ₂ O	53.61	4.34	16.34	20.69	53.92	4.24	16.67	20.54
9	C ₁₅ H ₁₄ N ₄ OCl ₂ ·0.05C ₆ H ₁₂	53.82	4.28	16.40	20.77	54.00	4.24	16.69	20.38
10	C ₁₅ H ₁₄ N ₄ OCl ₂ ·0.05H ₂ O	53.24	4.17	16.56	20.96	53.44	4.56	16.59	20.59
11	C ₁₈ H ₂₂ N ₄ O ₄ ·0.5H ₂ O	58.83	6.47	15.07		58.91	6.28	15.13	
12	C ₁₅ H ₁₃ N ₄ OCl ₃	48.48	3.53	15.08	28.62	48.40	3.68	14.92	28.74
13	C ₁₉ H ₁₈ N ₄ O·0.1H ₂ O	71.27	5.68	17.49		71.18	5.60	17.54	
14	C ₂₀ H ₂₀ N ₄ O ₂ ·0.25H ₂ O	68.01	5.81	15.87		67.90	5.63	15.92	
15	C ₂₁ H ₂₀ N ₄ O·0.4H ₂ O	71.73	5.96	15.93		71.76	5.97	15.81	
16	C ₂₂ H ₂₀ N ₄ O·0.15C ₆ H ₁₂	74.52	5.91	15.18		74.34	5.63	14.85	
17	C ₁₅ H ₁₄ N ₄ O	67.65	5.30	21.04		67.36	5.38	20.98	
18	C ₁₆ H ₁₆ N ₄ O ₂	64.37	5.67	19.71		64.23	5.72	19.66	
19	C ₁₆ H ₁₆ N ₄ O ₂ ·0.25H ₂ O	63.82	5.48	18.61		64.15	5.56	18.58	
20	C ₁₅ H ₁₃ N ₄ OCl	59.91	4.36	18.36	11.79	59.97	4.41	18.62	11.91
21	C ₁₅ H ₁₃ N ₄ OCl	59.91	4.36	18.36	11.79	59.91	4.42	18.57	11.69
22	C ₁₅ H ₁₃ N ₄ OCl	59.91	4.36	18.36	11.79	59.89	4.37	18.45	11.83
23	C ₁₇ H ₁₈ N ₄ O ₃	62.57	5.56	17.17		62.47	5.57	17.03	
24	C ₁₇ H ₁₈ N ₄ O ₃	62.57	5.56	17.17		62.29	5.53	16.96	
25	C ₁₇ H ₁₈ N ₄ O ₃	62.57	5.56	17.17		62.38	5.59	17.21	
26	C ₁₅ H ₁₂ N ₄ OCl ₂	53.75	3.61	16.72	21.15	53.60	3.62	16.63	20.97
27	C ₁₅ H ₁₂ N ₄ OCl ₂	53.75	3.61	16.72	21.15	53.83	3.60	16.60	21.01
27a	C ₁₅ H ₁₂ N ₄ OCl ₂	53.75	3.61	16.72	21.15	53.77	3.73	16.64	21.02
28	C ₁₅ H ₁₂ N ₄ OCl ₂	53.75	3.61	16.72	21.15	53.49	3.69	16.67	20.91
29	C ₁₈ H ₂₀ N ₄ O ₄	60.66	5.66	15.72		60.37	5.72	15.60	
30a	C ₁₅ H ₁₁ N ₄ OCl ₃	48.74	3.00	15.16	28.77	48.61	3.07	15.00	28.88
30b	C ₁₅ H ₁₁ N ₄ OCl ₃	48.74	3.00	15.16	28.77	48.63	3.09	15.03	28.67
31	C ₁₉ H ₁₆ N ₄ O·0.25H ₂ O	71.08	5.19	17.45		71.10	5.20	17.36	
32	C ₁₉ H ₁₆ N ₄ O	72.13	5.10	17.71		71.96	5.04	17.52	
33	C ₂₀ H ₁₈ N ₄ O ₂	69.35	5.24	16.17		69.44	5.29	16.30	
34	C ₂₁ H ₁₈ N ₄ O	73.67	5.30	16.36		73.37	5.23	16.41	
35	C ₂₂ H ₁₈ N ₄ O	74.14	5.01	15.76		73.97	5.23	15.61	

References and notes

- Folkman, J. Tumor Angiogenesis: therapeutic implication. *New Eng. J. Med.* **1971**, *285*, 1182–1186.
- Folkman, J. *Breast Cancer Res. Treat.* **1995**, *36*, 109–118.
- Bohle, A. S.; Kalthoff, H. Molecular mechanisms of tumor metastasis and angiogenesis. *Langenbecks Arch. Surg.* **1999**, *384*, 133–140.
- Hanahan, D.; Folkman, J. Patterns and emerging mechanism of the angiogenic switch during tumorigenesis. *Cell* **1996**, *196*, 353–364.
- Fox, S. B.; Harris, A. L. Diagnostic and prognostic significance of tumor angiogenesis. In *The New Angiotherapy*; Fan, T. P., Kohn, E. C., Eds.; Humana Press: Totowa, NJ, 2002, pp 151–176.
- Cherrington, J. M.; Strawn, L. M.; Shawver, L. K. New paradigms for the treatment of cancer: the role of anti-angiogenesis agents. *Adv. Can. Res.* **2000**, *20*, 1–38.
- Sun, L.; McMahon, G. Inhibition of tumor angiogenesis by synthetic receptor tyrosine kinase inhibitors. *Drug Discov. Today* **2000**, *5*, 344–353.
- Shauver, L. K.; Lipson, K. E.; Fong, T. A. T.; McMahon, G.; Strawn, L. M. Receptor tyrosine kinases in angiogenesis. In *The New Angiotherapy*; Fan, T. P., Kohn, E. C., Eds.; Humana Press: Totowa, NJ, 2002, pp 409–452, and references therein.
- Shin, D. M.; Ro, J. Y.; Hong, W. K.; Hittelamn, W. N. Dysregulation of epidermal growth factor receptor expression in premalignant lesions during head and neck tumorigenesis. *Cancer Res.* **1994**, *54*, 3153–3159.

10. Tateishi, M.; Ishida, T.; Mitsudomi, T.; Kaneko, S.; Sugimachi, K. Immunohistochemical evidence of autocrine growth factors in adenocarcinoma of the human lung. *Cancer Res.* **1990**, *50*, 7077–7080.
11. Gorgoulis, V.; Aninos, D.; Mikou, P.; Kanavaros, P.; Karameris, A.; Joardanoglu, J.; Rasidakis, A.; Veslemes, M.; Ozanne, B.; Spandidos, D. A. Expression of EGF, TGF- α and EGFR in squamous cell lung carcinomas. *Anticancer. Res.* **1992**, *12*, 1183–1187.
12. Fleming, T. P.; Saxena, A.; Clark, W. C.; Robertson, J. T.; Oldfield, E. H.; Aaronson, S. A.; Ali, I. U. Amplification and/or overexpression of platelet-derived growth factor receptors and epidermal growth factor receptor in human glial tumors. *Cancer Res.* **1992**, *52*, 4550–4553.
13. Maxwell, M.; Naber, S. P.; Wolfe, H. J.; Galanopoulos, T.; Hedley-Whyte, E. T.; Black, P. M.; Antoniades, H. N. Coexpression of platelet-derived growth factor (PDGF) and PDGF-receptor genes by primary human astrocytomas may contribute to their development and maintenance. *J. Clin. Invest.* **1990**, *86*, 131–140.
14. Hermanson, M.; Funa, K.; Hartman, H.; Claesson-Welsh, L.; Heldin, C.-H. Platelet-derived growth factor and its receptors in human glioma tissue: expression of messenger RNA and protein suggests the presence of autocrine and paracrine loops. *Cancer Res.* **1992**, *52*, 3213–3229.
15. Ross, J. S.; Fletcher, J. A. The HER2/neu oncogene in breast cancer: prognostic factor predictive factor and target for therapy. *Stem Cells* **1998**, *16*, 413–428.
16. Benjamin, L. E.; Keshet, E. Conditional switching of vascular endothelial growth factor (VEGF) expression in tumors: induction of endothelial cell shedding and regression of hemangioblastoma-like vessels by VEGF withdrawal. *Proc. Natl. Acad. Sci. USA* **1997**, *94*, 8761–8766.
17. Benjamin, L. E.; Golijanin, D.; Itin, A.; Pode, D.; Keshet, E. Selective ablation of immature blood vessels in established human tumors follows vascular endothelial growth factor withdrawal. *J. Clin. Invest.* **1999**, *103*, 159–165.
18. Burns, C.; Liu, W.; Shaheen, R.; Davis, D.; McConkey, D.; Wilson, M.; Bucana, C.; Hicklin, D.; Ellis, L. Vascular endothelial growth factor is an in vivo survival factor for tumor endothelium in a murine model of colorectal liver metastases. *Cancer (Phila.)* **2000**, *89*, 488–499.
19. Carmeliet, P.; Dor, Y.; Herbert, J. M.; Fukumura, D.; Brusselmans, K.; Dewerchin, M.; Neeman, M.; Bono, F.; Abramovitch, R.; Maxwell, P.; Koch, C. J.; Ratcliffe, P.; Moons, L.; Jain, R. K.; Collen, D.; Keshet, E. Role of HIF-1 α in hypoxia-mediated apoptosis cell proliferation and tumour angiogenesis. *Nature (Lond.)* **1998**, *394*, 485–490.
20. Gerber, H. P.; McMurtrey, A.; Kowalski, J.; Yan, M.; Keyt, B. A.; Dixit, V.; Ferrara, N. Vascular endothelial growth factor regulates endothelial cell survival through the phosphatidylinositol 3'-kinase/AKT signal transduction pathway. *J. Biol. Chem.* **1998**, *273*, 30336–30343.
21. Gerber, H. P.; Dixit, V.; Ferrara, N. Vascular endothelial growth factor induces expression of the antiapoptotic proteins Bcl-2 and A1 in vascular endothelial cells. *J. Biol. Chem.* **1998**, *273*, 13313–13316.
22. Holash, J.; Wiegand, S. J.; Yancopoulos, G. D. New model of tumor angiogenesis: dynamic balance between-vessel regression and growth mediated by angiopoietins and VEGF. *Oncogene* **1999**, *18*, 5356–5362.
23. Jain, R. K.; Safabakhsh, N.; Sckell, A.; Chen, Y.; Jiang, P.; Benjamin, L.; Yuan, F.; Keshet, E. Endothelial cell death angiogenesis and microvascular function after castration in an androgen-dependent tumor: role of vascular endothelial growth factor. *Proc. Natl. Acad. Sci. USA* **1998**, *95*, 10820–10825.
24. Shaheen, R. M.; Tseng, W. W.; Davis, D. W.; Liu, W.; Reinmuth, N.; Vellagas, R.; Wiczorek, A. A.; Ogura, Y.; McConkey, D. J.; Drazan, K. E.; Bucana, C. D.; McMahon, G.; Ellis, L. M. Tyrosine kinase inhibition of multiple angiogenic growth factor receptors improves survival in mice bearing colon cancer liver metastases by inhibition of endothelial cell survival mechanisms. *Cancer Res.* **2001**, *61*, 1464–1468.
25. Levitt, M. L.; Koty, P. P. Tyrosine kinase inhibitors in preclinical development. *Invest. New Drugs* **1999**, *17*, 213–226.
26. Rusnak, D. W.; Lackey, K.; Affleck, K.; Wood, E. R.; Alligood, K. J.; Rhodes, N.; Keith, B. R.; Murray, D. M.; Knight, W. B.; Mullin, R. J.; Gilmer, T. M. The Effects of the novel, reversible epidermal growth factor receptor/ ErbB-2 tyrosine kinase inhibitor GW2016 on the growth of human normal and tumor-derived cell lines in vitro and in vivo. *Mol. Cancer Therap.* **2001**, *1*, 86–94.
27. Traxler, P.; Bold, G.; Buchdunger, E.; Caravatti, G.; Furet, P.; Manley, P.; O'Reilly, T.; Wood, J.; Zimmermann, J. Tyrosine kinase inhibitors: from rational design to clinical trials. *Med. Res. Rev.* **2001**, *21*, 499–512.
28. Traxler, P.; Furet, P. Strategies toward the design of novel and selective protein tyrosine kinase inhibitors. *Pharmacol. Ther.* **1999**, *82*, 195–206.
29. Fry, D. W. Protein tyrosine kinases as therapeutic targets in cancer chemotherapy and recent advances in the development of new inhibitors. *Exp. Opin. Invest. Drugs* **1994**, *3*, 577–595.
30. Dancey, J.; Sausville, E. A. Issues and progress with protein kinase inhibitors for cancer treatment. *Nat. Rev. Drug Discov.* **2003**, *2*, 296–313.
31. Kerbel, R.; Folkman, J. Clinical translation of angiogenesis inhibitors. *Nat. Rev. Cancer* **2002**, *2*, 727–739.
32. Gangjee, A.; Elzein, E.; Kothare, M.; Vasudevan, A. Classical and nonclassical antifolates as potential antitumor, antipneumocystis and antitoplasma agents. *Curr. Pharm. Des.* **1996**, *2*, 263–280.
33. Rosowsky, A. In *Progress in Medicinal Chemistry*; Ellis, G. P., West, G. B., Eds.; Elsevier Science B.V.: Amsterdam, 1989; 26, pp 1–252.
34. Longo-Sorbello, G. S. A.; Bertino, J. R. Current understanding of methotrexate pharmacology and efficacy in acute leukemias. Use of newer antifolates in clinical trials. *Haematologica* **2001**, *86*, 121–127.
35. Bergers, G.; Song, S.; Meyer-Morse, N.; Bergsland, E.; Hanahan, D. Benefits of targeting both pericytes and endothelial cells in the tumor vasculature with kinase inhibitors. *J. Clin. Invest.* **2003**, *111*, 1287–1295.
36. Erber, R.; Thurnher, A.; Katsen, A. D.; Groth, G.; Kerger, H.; Hames, H.-P.; Menger, M. D.; Ullrich, A.; Vajkoczy, P. Combined inhibition of VEGF and PDGF signaling enforces tumor vessel regression by interfering with pericyte-mediated endothelial cell survival mechanisms. *FASEB J.* **2004**, *18*, 338–340.
37. (a) Gangjee, A.; Zeng, Y.; McGuire, J. J.; Kisliuk, R. L. Effect of c9-methyl substitution and C8-C9 conformational restriction on antifolate and antitumor activity of classical 5-substituted 24-diaminofuro[2,3-d]pyrimidines. *J. Med. Chem.* **2000**, *43*, 3125–3133; (b) Harris, N. V.; Smith, C.; Bowden, K. Antifolate and antibacterial activities of 6-substituted 24-diaminoquinazolines. *Eur. J. Med. Chem.* **1992**, *27*, 7–18.
38. McTigue, M. A.; Wichersham, J. A.; Pinko, C.; Showalter, R. E.; Parast, C. V.; Tempczyk-Tussell, A.; Gehring, M. R.; Mroczkowski, B.; Kan, C. C.; Villafrance, J. E.; Applelt, K. Crystal structure of the kinase domain of human vascular endothelial growth factor receptor 2: a key enzyme in angiogenesis. *Structure (Lond.)* **1999**, *7*, 319.
39. Tripos Inc., 1699 South Handley Road, Suite 303, St. Louis, MO 63144.

40. Hubbard, S. R. Crystal structure of the activated insulin receptor tyrosine kinase in complex with peptide substrate and ATP analog. *EMBO J.* **1997**, *16*, 5573–5581.
41. Gangjee, A.; Yang, J.; Ihnat, M. A.; Kamat, S. Antiangiogenic and antitumor agents: design synthesis and evaluation of novel 2-amino-4-(3-bromoanilino)-6-benzylsubstituted pyrrolo[2,3-*d*]pyrimidines as inhibitors of receptor tyrosine kinases. *Bioorg. Med. Chem.* **2003**, *11*, 5155–5170.
42. Cody, V.; Luft, J. R.; Pangborn, W.; Gangjee, A. Analysis of three crystal structure determinations of 5-methyl-6-*n*-methylanilino pyridopyrimidine antifolate complex with human dihydrofolate reductase. *Acta. Crystallogr. D* **2003**, *59*, 1603–1609.
43. Carey, F. A.; Sundberg, R. J. *Advanced organic chemistry Part B: reactions and synthesis*; Plenum Press: New York, London, 1990.
44. (a) Bestmann, H. J.; Vostrowsky, O. Selected topic of wittig reaction in the synthesis of natural products In *Topics in Current Chemistry*; Boschke, F. L., Ed.; Springer-Verlag press: Berlin Heidelberg, New York, 1983; vol. 109, pp 85–164(b) The IC₅₀ value of any compound against any RTK varies significantly depending upon the assay conditions used. The literature is surfeit with different values for the IC₅₀ of, for example SU5416, against VEGFR-2 TK, depending on the assay used: (1) Sun et al., Design, synthesis and evaluations of substituted 3-[(3- or 4-carboxyethylpyrrol-2-yl)methylidene]indolin-2-ones as inhibitors of VEGF, FGF and PDGF receptor tyrosine kinases, *J. Med. Chem.*, **1999**, *42*, 5120–5130. This is a publication from SUGEN, the company which discovered SU5416, which reports an IC₅₀ for SU5416 of 0.7 μM for VEGFR-2 TK Table 3, page 5122 (compound 2 in the manuscript) and suggests a value of IC₅₀ = 1.04 μM from Ref. 5 (Sun et al., *J. Med. Chem.*, **1998**, *41*, 2588–2603 also from SUGEN); (2) Fong et al. SU5416 is a potent inhibitor of the vascular endothelial growth factor receptor (Flk-1/KDR) that inhibits tyrosine kinase catalysis, tumor vascularization and growth of multiple tumor types, *Cancer Res.*, **1999**, *59*, 99–106. This is also a publication from SUGEN and lists an IC₅₀ value of 1.04 ± 0.53 μM for the inhibition of VEGF-dependent phosphorylation of the Flk-1 receptor in Flk-1-over-expressing NIH 3T3 cells. This was an ELISA-based assay (page 101 of this reference), similar to our ELISA-based assay. Further, this reference evaluated SU5416 as an inhibitor of autophosphorylation of Flk-1 receptor with an IC₅₀ of 1.23 μM using an ELISA-based biochemical kinase assay (page 101 of this reference). In HUVECs, SU5416 inhibited VEGF-driven mitogenesis at an IC₅₀ of 0.04 μM. This is an antiangiogenesis assay similar to our CAM assay and demonstrates the significant difference in VEGFR-2 assay and antiangiogenic assay systems to evaluate analogs. There are several other examples in the literature with different IC₅₀ values for SU5416. We believe that the IC₅₀ value depends upon the assay and several other parameters and the only way to meaningfully compare two or more compounds is to use a comparative standard in the same assay system as we have reported. Our value for SU5416 in the VEGFR-2 ELISA-based assay IC₅₀ of 2.4 μM is similar to that obtained in the references cited above from SUGEN itself and hence we believe are appropriate values. In addition, our IC₅₀ of 0.032 μM for the CAM assay for SU5416 is very close to the IC₅₀ for SU5416 against HUVECs assay of 0.04 μM in the reference cited above.
45. Gangjee, A.; Zeng, Y.; McGuire, J. J.; Kisliuk, R. L. Synthesis of *N*-[2-[1-ethyl-2-(2,4-diaminofuro[2,3-*d*]pyrimidin-5-yl)-ethyl]benzoyl]-L-glutamic acid as an antifolate. *J. Med. Chem.* **2002**, *45*, 1942–1948.
46. DeGraw, J. L.; Christie, P. H.; Kisliuk, R. L.; Gaumont, Y.; Sirotnak, F. M. Synthesis and antifolate properties of 9-alkyl-10-deazaminopterin. *J. Med. Chem.* **1990**, *33*, 212–215.
47. Soucy, N. V.; Ihnat, M. A.; Kamat, C. D.; Hess, L.; Post, M. J.; Klei, L. R.; Clark, C.; Barchowsky, A. Arsenic stimulates angiogenesis and tumorigenesis in vivo. *Toxicol. Sci.* **2003**, *76*, 271–279.
48. Fidler, I. J. Biological behavior of malignant melanoma cells correlated to their survival in vivo. *Cancer Res.* **1975**, *35*, 218–224.
49. Fidler, I. J.; Gersten, D. M.; Budmen, M. B. Characterization in vivo and in vitro of tumor cells selected for resistance to syngeneic lymphocyte-mediated cytotoxicity. *Cancer Res.* **1976**, *36*, 3160–3165.
50. Fidler, I. J.; Nicolson, G. L. Tumor cell and host properties affecting the implantation and survival of blood-borne metastatic variants of B16 melanoma. *Isr. J. Med. Sci.* **1978**, *14*, 38–50.
51. Poste, G.; Doll, J.; Hart, I. R.; Fidler, I. J. In vitro selection of murine B16 melanoma variants with enhanced tissue-invasive properties. *Cancer Res.* **1980**, *40*, 1636–1644.
52. Wilson, S. M.; Barsoum, M. J.; Wilson, B. W.; Pappone, P. A. Purine nucleotides modulate proliferation of brown fat preadipocytes. *Cell Prolif.* **1999**, *32*, 131–140.
53. Vu, M. T.; Smith, C. F.; Burger, P. C.; Klintworth, G. K. An evaluation of methods to quantitate the chick chorioallantoic membrane assay in angiogenesis. *Lab. Invest.* **1985**, *53*, 499–508.
54. Sheu, J. R.; Fu, C. C.; Tsai, M. L.; Chung, W. J. Effect of U-995 a potent shark cartilage-derived angiogenesis inhibitor on anti-angiogenesis and anti-tumor activities. *Anticancer Res.* **1998**, *18*, 4435–4441.
55. Brooks, P. C.; Montgomery, A. M.; Cheresch, D. A. Use of the 10-day old chick embryo model for studying angiogenesis. *Methods Mol. Biol.* **1999**, *129*, 257–269.
56. Marks, M. G.; Shi, J.; Fry, M. S.; Xiao, Z.; Trzyna, M.; Pokala, V.; Ihnat, M. A.; Li, P.-K. Effects of putative hydroxylated thalidomide metabolites on blood vessel density in the chorioallantoic membrane (CAM) and on tumor and endothelial cell proliferation. *Biol. Pharm. Bull.* **2002**, *25*, 597–604.